High Dispersion Observations of Venus During 1972

The CO_2 band at 7820Å

by

L. D. Gray Young
A. T. Young
Physics Department
Texas A&M University
College Station, Texas 77843

and

A. Woszczyk
Astronomical Observatory
Nicholas Copernicus University
Torun, Poland

Report No 15

The research described in this report was
funded by the

National Aeronautics and Space Administration

Contract No. NGR 44-001-117

Department of Physics
Texas A & M University
College Station, Texas 77843

January 31, 1975

A paper based on the material in this report has been submitted to Icarus.

(NASA-CR-142023) HIGH DISPERSION OBSERVATIONS OF VENUS DURING 1972. THE CO2 BAND AT 7820 ANGSTROM (Texas A&M Univ.) 56 p HC $4.25 CSCL 03A
N75-16437
Unclas
G3/89 08924

PRECEDING PAGE BLANK NOT FILMED

Abstract

Forty-seven well-exposed photographic plates of Venus which show the spectrum of the carbon dioxide band at 7820Å were obtained at Table Mountain Observatory in September-October 1972. These spectra showed a semi-regular 4-day variation in the CO_2 abundance over the disk of the planet (Young et. al. 1974). We also find evidence for temporal variations in the rotational temperature of this band and temperature variations over the disk. The two quantities, CO_2 abundance and temperature, do not show any obvious relationship; however, an increase in the temperature usually is accompanied by a decrease in the abundance of CO_2. The average temperature, found from a curve of growth analysis assuming a constant CO_2 line of width, is 249 ± 1.4°K (one standard deviation). This temperature is noticeably higher than the rotational temperature of 242 ± 2°K found for this same band in 1967 (Schorn et. al. 1969) and of 242 ± 1.2°K in 1968-9 (Young et. al. 1971).

I. Introduction

For the past 9 years there has been a spectroscopic patrol of Venus, to monitor the apparent abundance of carbon dioxide visible in reflected sunlight abover her cloud tops and to measure the rotational temperature of the CO_2 (See Young, 1972). This patrol began, and continues, at McDonald Observatory; observations have also been made more recently at Table Mountain Observatory. The 24-inch telescope at Table Mountain provides a relatively small image of the planet, compared to that of either the 82-inch or 107-inch telescopes at McDonald Observatory. As a result the Table Mountain observations were mainly intended to monitor daily changes at a few standard slit positions; areal coverage over the planet was restricted. On the other hand, the dispersion of the plates obtained at Table Mountain (1.6Å/mm) was somewhat higher than that of the best plates previously obtained at McDonald Observatory (~2Å/mm).

In September of 1972, an intensive spectroscopic patrol of Venus was simultaneously undertaken at both Table Mountain and McDonald Observatories. These observations were made in cooperation with the Paris, New Mexico State University and Lowell Observatories, where ultraviolet photographs of cloud marking were taken. This was the first extensive effort made to observe Venus in both the ultraviolet and infrared regions of the spectrum over a fairly long time interval (3 weeks). One difficulty, in the past, had been the comparative lack of overlap of the dates of observation for the planetary patrols in the two spectral regions. This paper will only be concerned with the results of the Table Mountain observations of the CO_2 band at 7820Å. When the results from the other observations are published, we shall see if any correlation exists between our results and theirs.

2. Observations and Measurements

The spectrograms used in this study are listed in Table 1. The plate number is given in column 1. When more than one spectrum was taken on one plate (as was usually the case, to conserve plates) successive spectra are denoted by the suffixes a, b, and c. The spectra were taken at the coudé focus of the 24-inch telescope. The spectrograph has been described by Young and Young (1972). The 7820Å spectra were taken in 4th order (1.6Å/mm) through a RG-715 filter. A typical exposure time of 30 minutes was required. Columns 2 and 3 of Table 1 give the date and time of the observations. Column 4 gives the slit orientation. We have followed the numbering scheme of Schorn et. al. (1969) to indicate the six standard* slit positions used in this set of observations: 1) pole-to-pole near the terminator; 2) pole-to-pole near the limb; 3) parallel to the equator near the South Pole; 4) parallel to the equator near the sub-Earth Point; 5) parallel to the equator near the North pole; 6) Parallel to the line joining the cusps and midway between limb and terminator. The last position of the slit was adopted as "standard" because it produced spectra of the greatest width and uniformity. On days when local weather conditions were such that it appeared we would be lucky to get one spectrum of Venus, we always used this "standard" slit position. Our seeing estimates are given in Column 5 (for comparison we note that the diameter of Venus during this period was about 18 seconds of arc).

---

* In Table 5, a slightly more refined scheme is used to indicate the slit position on Venus. The information given in Table 1 is meant to facilitate a comparison of the present results with those of Schorn et. al. (1969).

In our preliminary paper, (Young et. al., 1974) the photographic and photometric procedures we used were described in great detail. In summary, all the Table Mountain spectra were taken on ammonia-hypersensitized IV-N plates, developed for 14 minutes in D-76 with vigorous agitation. Spot plates were taken at the same time, for the same length of exposure, and developed with the Venus plates. The spectra were traced in the density mode, which for IV-N plates amounts to a direct intensity tracing.

All three authors measured the heights (in mm) of 11 solar lines and 25 CO_2 lines for each tracing of a Venus spectrum. The average sum of the heights of the solar lines in mm, is given in Column 6. Column 7 gives the ratio, R, of the average sum of the heights of the CO_2 lines (in mm) to the average sum of the heights of the solar lines (in mm). This quantity, R, was used in our preliminary paper as a measure of the relative abundance of CO_2. The main reason for using this ratio was to eliminate the uncertainty in the conversion from square counts to mÅ for the equivalent widths of the carbon dioxide lines. The heights of the CO_2 lines are directly proportional to their equivalent widths; the Venusian lines are narrow compared to the instrumental width so the apparent "line profile" is, in fact, the instrumental slit function.

On the other hand, the solar lines are generally much broader than the slit width and their line shape is usually well resolved. Whether or not the solar lines were completely resolved does not affect the CO_2 abundance ratio for the following reason: All the Venus plates were taken with an identical slit width for the spectrograph and were always traced using the same slit width for the microdensitometer. Thus the ratios, R, were all affected by the same instrumental effects, and are "good" measures of the CO_2 abundance variations. Obviously the choice of different instrumental parameters would affect the numerical value of the ratios, but not their usefulness in sensing small changes in the CO_2 abundance.

Because the height of the CO_2 lines is directly proportional to their equivalent width, one can use these heights directly to obtain the rotational temperature for a particular spectrum. And that is what was done in this paper. However, in order to compare these results with other measurements on the 7820Å band, it is necessary to convert the heights of the CO_2 lines to equivalent widths in mÅ. This calibration was done using the solar lines given in Table II. We have used the equivalent widths of the solar lines given by Moore et. al. (1966), out of necessity, but the equivalent widths measured by Barker and Perry for integrated sunlight are in fact the appropriate ones for our Venus spectra. As can be seen from Table II, the average rms difference in the two measurements of solar equivalent widths is 13.4 percent, while the difference in the sum of the five lines is 208.2 - 209.0 mÅ or only 0.4 percent. Our usual calibration procedure has been to use the average of the conversion factors (from mm^2 of chart paper to mÅ) found from the sum of the solar lines and that obtained from the individual solar lines. In view of Barker and Perry's new measurements, it would appear that the conversion factor obtained from the sum of the equivalent widths is the better one to use. This sum equals 429mÅ for the solar calibration lines given in Table II. Table I gives the sum of the heights of these solar lines for each plate. The equivalent width of a Venus line is given by

$$W_{♀} = h_{♀} (b_{♀}/b_{\odot})(\Sigma W_{\odot}/\Sigma h_{\odot}), \qquad (1)$$

where h is the height of the line and b is the base of a triangular shaped line of equivalent width W. The ratio $(b_{♀}/b_{\odot}) \approx 2/3$ for our data.

III Determination of Rotational Temperatures and other parameters.

The rotational temperature can be found if we assume that the curve of growth can be locally approximated by a straight line of slope, b, i.e.

$$W(m) \propto S(m)^b \qquad (2)$$

where m is the rotational line index. The index m is related to the rotational quantum number of the lower state, J", by $m = -J''$ for the P branch of a band and $m = J'' + 1$ for the R branch. The intensity of a rotational line in the 7820Å band of CO_2 is given by

$$S(m) = (S_v/Q_{rot})|m|\exp(-hcBm(m-1)/kT) \quad (3)$$

where S_v is the band intensity (equal to the sum of the individual rotational line intensities), Q_{rot} is the rotational partition function, $(hcB/k) = 0.5614$ for this band and T is the rotational temperature. From equations (2) and (3) we see that

$$\ln[W(m)/m^b] = \ln W_o - [0.5614m\ (m-1)b/T]$$

where W_o corresponds to the equivalent width of the RO line; depending upon the pressure, temperature and amount of absorbing gas where the lines are formed, W_o will be a function of the amount of absorbing gas and may also be a function of the effective pressure for line formation, etc.

In a linear least-squares fit to (4), the rotational temperature is determined for a particular value of b; the quantity W_o is merely the intercept of this line, and it will be equal to the measured equivalent width of the RO CO_2 line only if the best fit to all the CO_2 lines in the band goes through RO. However, W_o is a convenient measure of the CO_2 abundance.

For historical reasons, we first compute the rotational temperature assuming a square-root absorption law, b = 0.5. The results of these computations are given in Column 2 of Table 3, for each of the three authors' measurements. The individuals are identified by a single initial following the plate number given in Column 1: G = LDGY, Y = ATY, and W = AW. In Column 3, the quantity W_o is given; this has been converted to mÅ by the calibration scheme discussed previously. In Figs. 1 to 16 each individual's measurements of the heights of the Venus lines, in mm, are shown. We have done this in preference to converting these heights to mÅ, because we have come to doubt the accuracy of our absolute calibration and believe the relative measurements are more accurate. In Column 4 we give the percentage standard deviation in the heights (or equivalent widths) as found from the square-root curve of growth temperature fit.

The assumption of a square-root absorption law is the first in a series of iterations where b and hence T(b) are allowed to vary. The quantity T_o (given in Column 9 of Table 3) is the temperature for which line intensities are computed from equation (3) to be used for the curve of growth indicated by equation (2). As an example of how this iterative scheme works, we show, in Table 4, the intermediate results found for a typical plate.

The first column of Table 4 shows what happens when we assume T_o = 240°K. Columns 2 to 4 give the temperatures found from each author's measurements of plate T660B. Columns 5 to 7 give the standard deviation of the heights (or equivalent width) obtained from the temperature fit: Columns 8 to 11 give the differences between T(b) and the assumed value of T_o. The values of T(b) are seen to be higher than T_o, suggesting that T_o should be increased. When T_o is increased to 250°K, both the standard deviation in the heights and $\Delta T = T(b) - T_o$ decrease. At this point a familiar problem crops up. One person's measurements suggest that T_o should be increased further, while the other two individuals' measurements suggest it should be decreased slightly. We want to use the same value of T_o for any given spectrum and not allow it to vary from one person's measurments to another, since all three measurments are combined to find the average value of T(b) from a least-wquares fit to all the data. Increasing T_o from 250°K to 260°K gives a good fit to one person's measurments, but a poor fit to the measurments of the other two people. The temperature, T_o, which shows the minimum sum of the standard deviations (or ΔT) is chosen as the "best" value of T_o.

The values of b (the slope of the curve of growth) and T(b) are given in Columns 5 and 6 of Table 3. Column 7 gives $W_o(b)$, converted from heights to mÅ; the standard deviation of $W_o(b)$ is given in Column 8.

Table 5 summarizes our final results. The exact slit position for each spectrum is given in Column 2; the remainder of Table 5 resembles Table 3 in layout.

The histogram of the final temperatures, T(b), is shown in Fig. 17. We note that the external spread of the individual temperature determinations, σ_{ext}, is significantly larger than the average internal precision of a single temperature determination, σ_{int}, which is given by the least-squares solutions for T. These data are the first examples of a significant temperature spread detected in the 7820Å CO_2 band; earlier data (Young et al., 1971; Schorn et al., 1969) gave essentially equal values of σ_{int} and σ_{ext}.

At the end of Table 5 we give the errors in the mean found from both σ_{int} and σ_{ext} for each region on the planet. If σ_{ext} is markedly larger than σ_{int} for a region, a real variation in temperature is indicated. If σ_{ext} is less than σ_{int}, which usually happens only if a few spectra cover that region, the external agreement must be regarded as fortuitous, and the larger value (σ_{int}) must be taken as a more reliable estimate of the mean error. This is because σ_{int} is based on a large number of degrees of freedom (the number of measured lines) while σ_{ext} has only a few degrees of freedom (the number of spectra for a given region.) For this reason, we have based mean-error estimates on σ_{int} in the past. We find that the average temperature at the equator is slightly higher than temperature of the polar regions (and the average temperature over the planet). Since the temperatures found for regions of Venus where the slit was aligned parallel to the equator are slightly warmer than the temperatures found when the slit was aligned from pole-to-pole, this might suggest that the average temperature distribution over the planet consists of three warm zones (N. polar, equatorial and S. polar) separated by 2 cooler zones. The evidence for such a suggestion is rather weak, as can be seen from Table 6. The best data to compare with our present results are those of Young et al. (1971) for the 7820Å band and those of Schorn et al. (1974) for the 8689Å band; the other spectra were taken at lower dispersion, but are included in this comparison. With the exception of the present results and those of Young et al. (1969), the number of measurements (indicated in parentheses in Table 6) was usually much greater for the pole-to-pole observations than for those made with the slit aligned parallel to the equator. The temperature differences, weighted inversely by the error squared, indicate the average temperature in the equatorial and polar regions is 2.3°K higher than that near the limb or terminator.

From Table 5 we also find that greater than average amounts of CO_2 are found above the terminator and the north and south polar region; less than average amounts are found above the limb, equatorial and standard slit positions. Thus we do not find a correlation between higher than average amounts of CO_2 and higher than average rotational temperatures (as one would expect for almost any ordinary model atmosphere). If we ignore the limb and terminator results, because of the comparatively small number of measurements at these locations, the situation is not improved: A higher than average temperature (equatorial) region has a lower than average CO_2 abundance, but so does a lower than average temperature (standard slit position) region. Once again, we find no obvious relation between CO_2 abundance and temperature from our measurements of Venus.

Figure 18 shows the relation between the intercept of the linear least squares fits to the temperature, $W_o(0.5)$ and $W_o(b)$, and the CO_2 absorption ratio relative to the solar lines R. We see that $W_o(0.5)$ is probably a better measure of the CO_2 abundance than $W_o(b)$ since the former quantity shows less scatter as a function of R. Figure 19 shows the values of T as a function of the W_o. Since T(b) is believed to be the actual value of the rotational temperature and $W_o(0.5)$ the best measure of CO_2 abundance, this quantity is also shown. Once again, no relation between temperature and CO_2 abundance is obvious.

In Table 7 we give the differences $\Delta W_o(0.5) = (W_o(0.5)_i - \bar{W}_o(0.5)_i)$ and $\Delta T(b) = (T(b)_i - \bar{T}(b)_i)$, where i refers to the region on Venus; these are shown as a function of date in Figure 20. While there was no obvious correlation between temperatures and CO_2 abundances, it appears that these differences are correlated in the sense that positive values of ΔW correspond to negative values of ΔT. That is to say that $\frac{dT}{dW} < 0$ (or $\frac{dT}{dP} < 0$, since W is related to the abundance and hence the pressure, since CO_2 is a major, uniformly mixed constituent of the Venus atmosphere). This result implies that the region of the atmosphere we are observing is stable; since the warmer layers of the atmosphere are presumably at higher altitudes no convection is expected. Yet we observe quite considerable temporal variations in the temperature and, to a somewhat lesser extent, variations in the CO_2 abundance.

IV. Conclusions

We appear to be seeing real temperature variations in the atmosphere of Venus, as well as indications that the CO_2 abundance above the cloud tops (or optical depth $\tau \sim 1$) varies. The values of these two quantities do not appear to be related; however, the derivatives of these quantities with respect to time, $\frac{dT}{dt}$ and $\frac{dW}{dt}$ appear to be related by $\frac{dT}{dt} = -C\,\frac{dW}{dt}$, where C is presumably a constant. The average temperature (249±1.4°K) found for this set of observations appears to be somewhat higher than the average temperature (242±2°K) found in the past (Young, 1972) for series of observations extending over a longer time period. It will be of some interest to compared our results with those obtained at McDonald Observatory during the same time period, when the latter become available.

IV. Acknowledgement

This researhc was supported in part by the scientific exchange program of the American and Polish National Academies of Science, and in part by the National Aeronautics and Space Administration under contract Number NGR 44-001-117 at Texas A&M University.

References

E. S. Barker and M. A. Perry (1974), "Solar Equivalent Widths (Integrated Disk) for P-Branch Region of the 7820Å CO_2 and 8689Å Bands". McDonald Observatory.

C. E. Moore, M. G. J. Minnaert, and J. Houtgast, (1966), "The Solar Spectrum 2935Å to 8770Å". Monograph 61, National Bureau of Standards, Washington, D.C.

R. A. Schorn, L. D. Gray, and E. S. Barker, (1969), High Dispersion Observations of Venus. III. The Carbon Dioxide Band at 7820Å" Icarus 10, 241-257.

R. A. J. Schorn, A. Woszczyk, and L. D. G. Young, (1974), High Dispersion Observations of Venus During 1968 and 1969 II. The Carbon Dioxide Band at 8689Å" Icarus (to be published).

R. A. Schorn, L. G. Young, and E. S. Barker, (1970), High Dispersion Spectroscopic Observation of Benus VI. The Carbon Dioxide Band at 10362Å" Icarus 12, 391-402.

R. A. Schorn, L. G. Young, and E. S. Barker, (1971), VIII The Carbon Dioxide Band at 10627Å" Icarus 14, 21-35.

A. T. Young, A. Woszczyk, and L. G. Young, (1974), "Spectroscopic Observations of Spatial and Temporal Variations on Venus", Acta Astron. 24, 55-68.

A. T. Young and L. G. Young, (1972), "OBserving Venus near the Sun" Sky and Tel. 43, 140-144.

L. D. G. Young, (1972), "High Resolution Spectra of Venus - A Review" Icarus 17, 632-658.

L. D. G. Young, R. A. J. Schorn, E. S. Barker, (1970), High Dispersion Spectroscopic Observations of Venus. VIII. The Carbon Dioxide Band at 10488Å" Icarus 13, 58-73.

L. D. G. Young, R. A. J. Schorn, E. S. Barker, and M. MacFarlane, (1969), High Dispersion Spectroscopic Observations of Venus V. The Carbon Dioxide Band at 8689Å" Icarus 11, 390-407.

L. D. G. Young, R. A. J. Schorn, E. S. Barker, and A. Woszczyk, (1971), High Dispersion Spectroscopic Observations of Venus during 1968 and 1969. I. The Carbon Dioxide Bands at 7820Å and 7883Å' Acta Astron. 21, 329-363.

L. G. Young, A. T. Young, J. W. Young, and J. T. Bergstralh, (1973), "The Planet Venus: A New Periodic Spectrum Variable" Astrophys. J., 181, L5-L8.

List of Figures

Table I
Spectrograms Studied

Plate	Date	Time of observation U. T.	Slit Orientation	Seeing Sec. of arc	$\Sigma h_{\odot}$, Height of solar lines, mm	R, Ratio of CO_2 to solar lines
T622	17 IX 72	13:06-13:36	6	1-3	228.7	2.04
T624a	17 IX 72	17:15-17:50	1	2-6	208.0	2.13
T624b	17 IX 72	17:52-18:27	2	2-6	208.3	2.00
T625a	18 IX 72	12:56-13:26	6	3-6	244.7	2.09
T625b	18 IX 72	14:06-14:36	3	3-6	219.0	2.15
T625c	18 IX 72	14:38-15:08	5	3-6	237.7	2.18
T627a	19 IX 72	14:58-14:28	6	4-10	414.7	1.97
T630a	20 IX 72	14:51-15:21	6	1-2	263.0	1.96
T630b	20 IX 72	15:26-15:56	5	1-2	220.0	1.89
T630c	20 IX 72	15:58-16:33	5	1-2	170.0	2.17
T631a	20 IX 72	16:45-17:05	4	2-3	242.0	1.89
T631b	20 IX 72	17:05-17:35	3	2-3	250.3	2.01
T633a	21 IX 72	14:52-15:22	6	2-3	253.7	2.07
T633b	21 IX 72	15:45-16:15	4	2-3	258.7	1.98
T636a	23 IX 72	14:20-15:10	6	2-4	295.0	1.94
T636b	23 IX 72	15:16-16:08	3	1-3	276.7	2.03
T636c	23 IX 72	16:11-17:01	5	5-7	284.7	1.93
T640a	25 IX 72	14:31-15:01	6	2-4	254.3	2.15
T640b	25 IX 72	15:06-15:36	4	2-6	245.0	2.08
T640c	25 IX 72	15:40-16:10	3	4-8	262.7	2.04
T641a	25 IX 72	16:34-17:04	3	3-10	255.7	1.94
T641b	25 IX 72	17:27-17:57	3	3-10	253.7	1.96
T641c	25 IX 72	18:16-18:41	2	6-10	221.0	1.99
T644a	26 IX 72	14:19-15:09	6	2-4	279.7	1.97
T644b	26 IX 72	15:12-15:52	2	3-6	262.0	1.92
T644c	26 IX 72	15:55-17:15	1	4-6	172.7	2.01
T645a	26 IX 72	17:41-18:11	4	4-6	251.3	2.07
T645b	26 IX 72	18:28-18:58	5	5-10	179.3	2.04
T645c	26 IX 72	19:01-19:31	3	3-15	177.0	2.09
T647b	27 IX 72	15:01-15:31	4	1-3	240.3	1.86
T647c	27 IX 72	15:34-16:04	4	2-5	271.0	1.89
T648a	27 IX 72	16:10-16:40	3	2-5	216.0	1.97
T648b	27 IX 72	16:44-17:14	6	1-6	227.0	1.93
T649b	28 IX 72	18:21-18:59	6	5-20	243.0	1.91
T650b	30 IX 72	13:09-13:49	6	1-2	261.7	2.12

Plate	Date	Time of observation U. T.	Slit Orientation	Seeing Sec. of arc	Height of solar lines, mm	Ratio of CO_2 to solar lines
T650c	30 IX 72	13:52-14:22	4	1-2	239.0	2.13
T651a	30 IX 72	14:32-15:02	5	2	253.7	2.11
T651b	30 IX 72	15:05-15:35	3	2-5	225.0	2.16
T651c	30 IX 72	15:40-16:05	6	3-6	255.0	2.11
T654b	I X 72	16:53-17:23	6	2-7	269.0	1.84
T655b	2 X 72	13:17-13:52	6	10-20	263.7	1.91
T657b	3 X 72	13:46-15:27	6	3-10	266.3	1.99
T658b	4 X 72	13:27-14:08	6	5-10	240.3	2.07
T660b	5 X 72	12:56-13:27	6	1-2	268.0	1.98
T660c	5 X 72	13:33-14:03	4	1-3	226.7	1.86
T661b	7 X 72	14:17-14:56	6	1-3	251.0	1.93
T661c	7 X 72	15:03-15:31	4	1-3	217.7	2.11

Table 2
Solar Lines used for Intensity Calibration

Wavelength, Å	Equivalent Width, mÅ MMH*	BP**	ΔW, percent
7800.000	61	----	----
7802.51	12	----	----
7807.916	64	----	----
7835.317	42	43.8	4.1
7836.130	64	65.6	2.4
7849.984	66	54.9	-20.2
7855.405	25	29.9	16.4
7861.045	12	14.0	14.3
7863.799	15	----	----
7896.378	28	----	----
7912.870	40	----	----

* Moore et al. (1966)

** Barker and Perry (1974)

Table 3

Results of Analysis of the 1972 data for the 7820A
Band of Carbon Dioxide, assuming
a constant CO_2 line width

Plate Number		Square Root Absorption Law: T(0.5) °K	$W_o(0.5)$ mÅ	σ♀ Percent	b	Curve of Growth Absorption Law: T(b) °K	$W_o(b)$ mÅ	σ♀ Percent	T_o °K
T622	G	212^{220}_{240}	11.8	2.4	0.666	230^{236}_{225}	8.5	1.8	240
	Y	212^{221}_{204}	11.6	2.5	0.681	237^{242}_{232}	8.0	1.7	"
	W	220^{234}_{207}	11.0	3.6	0.718	238^{243}_{233}	7.5	1.6	"
average		214^{219}_{210}	11.3	1.2	0.677	236^{238}_{233}	8.0	0.9	240
T624a	G	213^{223}_{204}	12.1	2.7	0.640	238^{246}_{231}	9.1	2.1	240
	Y	225^{235}_{215}	11.5	2.6	0.605	240^{248}_{233}	9.3	2.1	"
	W	229^{241}_{219}	11.7	2.8	0.582	243^{252}_{235}	9.8	2.2	"
average		222^{228}_{216}	11.8	1.5	0.606	241^{245}_{236}	9.5	1.2	240
T624b	G	208^{224}_{194}	11.2	4.5	0.746	233^{241}_{227}	7.1	2.5	240
	Y	218^{240}_{200}	10.7	5.6	0.792	246^{253}_{239}	6.1	2.5	"
	W	202^{217}_{189}	11.2	4.5	0.773	232^{238}_{225}	6.6	2.6	"
average		209^{219}_{201}	11.0	2.8	0.779	238^{242}_{234}	6.5	1.5	240

Table 3 - Cont.
Page 2

Plate Number		T(0.5) °K	$W_o(0.5)$ mÅ	σ♀ Percent	b	T(b) °K	$W_o(b)$ mÅ	σ♀ Percent	T_o °K
T625a	G	253^{273}_{237}	10.9	3.7	0.682	262^{268}_{255}	7.9	1.8	260
	Y	238^{254}_{224}	11.0	3.6	0.760	265^{270}_{260}	6.4	1.5	"
	W	238^{254}_{224}	11.3	3.5	0.738	265^{271}_{259}	7.0	1.7	"
average		243^{252}_{234}	11.1	2.1	0.714	263^{267}_{259}	7.2	1.0	260
T625b	G	230^{243}_{218}	11.7	3.1	0.646	244^{250}_{238}	8.8	1.7	240
	Y	218^{231}_{206}	11.4	3.6	0.679	238^{245}_{232}	8.1	2.2	"
	W	235^{251}_{221}	11.1	3.5	0.649	249^{257}_{242}	8.4	2.2	"
average		227^{235}_{220}	11.5	2.0	0.655	243^{247}_{239}	8.5	1.2	240
T625c	G	220^{233}_{208}	12.4	3.3	0.690	237^{242}_{231}	8.7	1.8	240
	Y	225^{239}_{213}	11.7	3.5	0.691	244^{248}_{239}	8.1	1.5	"
	W	223^{233}_{213}	11.9	2.8	0.640	237^{242}_{232}	9.1	1.6	"
average		222^{229}_{216}	12.0	1.8	0.678	239^{243}_{236}	8.6	1.0	240
T627a	G	216^{229}_{204}	11.1	3.5	0.681	229^{235}_{223}	8.0	1.9	240
	Y	211^{225}_{199}	10.8	3.8	0.719	228^{233}_{222}	7.3	1.8	"
	W	226^{241}_{212}	10.6	3.8	0.703	244^{250}_{238}	7.2	1.7	"

Table 3 - Cont.
Page 3

Plate Number	T(0.5) °K	$W_o(0.5)$ mÅ	σ♀ Percent	b	T(b) °K	$W_o(b)$ mÅ	σ♀ Percent	T_o °K
G	218^{231}_{206}	10.9	3.6	0.694	232^{236}_{228}	7.6	1.5	240
W	225^{239}_{212}	10.1	3.5	0.693	239^{244}_{233}	7.0	1.6	"
average	219^{225}_{213}	10.8	1.6	0.703	235^{237}_{232}	7.4	0.8%	240
T630a G	231^{244}_{219}	10.6	3.1	0.656	246^{252}_{240}	8.0	1.7	240
Y	220^{236}_{206}	10.6	4.1	0.724	243^{249}_{238}	6.9	1.8	"
W	230^{242}_{219}	10.4	4.0	0.679	246^{253}_{240}	7.4	2.1	"
average	227^{235}_{219}	10.5	2.1	0.678	243^{246}_{239}	7.5	1.1	240
T630b G	248^{261}_{236}	10.4	2.8	0.601	268^{277}_{260}	5.1	2.0	260
Y	226^{248}_{208}	9.5	5.1	0.898	270^{276}_{264}	4.3	1.9	"
W	238^{260}_{218}	9.5	4.9	0.766	261^{268}_{254}	5.8	2.2	"
average	238^{250}_{227}	9.8	2.7	0.780	266^{272}_{261}	5.7	1.5	260
T630c G	227^{238}_{218}	12.9	2.6	0.544	252^{260}_{244}	11.8	1.7	250
Y	223^{235}_{211}	12.2	3.2	0.621	253^{263}_{244}	9.3	2.1	"
W	228^{238}_{218}	12.3	2.6	0.512	249^{259}_{240}	12.0	1.9	"
average	226^{232}_{220}	12.5	1.6	0.551	248^{254}_{243}	11.2	1.2	250

Table 3 - Cont.
Page 4

Plate Number		T(0.5) °K	$W_o(0.5)$ mÅ	$\sigma_♀$ Percent	b	T(b) °K	$W_o(b)$ mÅ	$\sigma_♀$ Percent	T_o °K
T631a	G	236^{246}_{226}	10.4	2.3	0.691	260^{265}_{256}	7.0	1.3	260
	Y	221^{233}_{209}	10.3	3.3	0.786	257^{263}_{251}	5.7	1.8	"
	W	225^{237}_{214}	10.2	3.1	0.760	259^{265}_{253}	6.0	1.7	"
average		227^{234}_{221}	10.3	1.7	0.733	260^{263}_{256}	6.4	1.0	260
T631b	G	237^{248}_{227}	11.0	2.4	0.514	233^{241}_{226}	11.0	2.0	240
	Y	239^{252}_{228}	10.6	2.9	0.605	252^{259}_{245}	8.6	1.8	"
	W	248^{259}_{237}	10.6	2.4	0.517	246^{254}_{238}	10.5	1.8	"
average		241^{248}_{235}	10.7	1.5	0.535	243^{248}_{238}	10.2	1.2	240
T633a	G	233^{241}_{226}	11.2	1.9	0.626	246^{251}_{242}	8.9	1.1	250
	Y	236^{248}_{226}	11.0	2.7	0.652	249^{255}_{243}	8.1	1.5	"
	W	216^{225}_{207}	11.2	2.6	0.716	238^{243}_{233}	7.4	1.6	"
average		228^{234}_{223}	11.2	1.4	0.658	245^{248}_{242}	8.3	0.8	250
T633b	G	241^{249}_{233}	11.2	1.8	0.590	254^{259}_{249}	9.3	1.3	250
	Y	227^{236}_{220}	11.0	2.0	0.663	250^{255}_{246}	7.9	1.2	"
	W	213^{222}_{206}	11.5	2.3	0.680	244^{249}_{239}	7.7	1.5	"
	G	224^{233}_{216}	11.2	2.2	0.658	251^{256}_{245}	8.0	1.5	"
	W	223^{232}_{214}	10.5	2.3	0.689	248^{253}_{243}	7.2	1.5	"

Table 3 - Cont.
Page 5

Plate Number		T(0.5) °K	$W_o(0.5)$ mÅ	σ♀ Percent	b	T(b) °K	$W_o(b)$ mÅ	σ♀ Percent	T_o °K
average		225^{229}_{222}	11.0	1.0	0.661	248^{250}_{246}	8.0	0.6	250
T636a	G	249^{262}_{238}	10.3	2.6	0.657	268^{274}_{262}	7.6	1.5	260
	Y	238^{252}_{226}	10.3	3.2	0.714	266^{271}_{261}	6.6	1.5	"
	W	242^{257}_{228}	10.5	2.9	0.717	260^{266}_{254}	6.8	1.5	"
average		238^{245}_{232}	10.5	1.6	0.704	264^{267}_{260}	6.9	0.9	260
T636b	G	226^{235}_{219}	10.9	2.1	0.680	247^{252}_{243}	7.6	1.3	250
	Y	238^{248}_{228}	10.3	2.3	0.673	256^{261}_{252}	7.3	1.4	"
	W	223^{231}_{215}	10.7	2.1	0.690	247^{251}_{243}	7.2	1.3	"
average		229^{234}_{224}	10.7	1.2	0.682	250^{253}_{248}	7.3	0.8	250
T636c	G	233^{243}_{223}	10.6	2.4	0.667	249^{253}_{246}	7.7	1.1	250
	Y	219^{227}_{211}	10.5	2.2	0.727	246^{251}_{242}	6.7	1.3	"
	W	216^{224}_{208}	10.5	2.2	0.731	246^{249}_{242}	6.6	1.1	"
average		222^{227}_{218}	10.5	1.3	0.714	248^{250}_{245}	6.9	0.7	250

Table 3 - Cont.
Page 6

Plate Number		T(0.5) °K	$W_o(0.5)$ mÅ	σ♀ Percent	b	T(b) °K	$W_o(b)$ mÅ	σ♀ Percent	T_o °K
T640a	G	226^{236}_{217}	12.0	2.4	0.628	237^{241}_{232}	9.5	1.4	240
	Y	223^{235}_{212}	11.6	3.0	0.660	238^{242}_{233}	8.6	1.4	"
	W	223^{235}_{212}	11.6	3.1	0.672	239^{244}_{234}	8.4	1.4	"
average		224^{230}_{218}	11.7	1.6	0.659	239^{242}_{236}	8.8	0.8	240
T640b	G	247^{262}_{234}	11.1	3.0	0.651	262^{271}_{254}	8.3	2.2	260
	Y	243^{256}_{230}	10.8	2.9	0.657	258^{266}_{251}	8.0	2.1	"
	W	247^{262}_{233}	10.7	3.2	0.667	261^{269}_{254}	7.8	2.1	"
	G	253^{274}_{235}	10.8	4.2	0.644	260^{273}_{248}	8.3	3.3	"
	Y	245^{260}_{241}	10.8	3.2	0.661	259^{266}_{251}	7.9	2.2	"
	W	252^{270}_{237}	10.2	3.6	0.633	266^{276}_{256}	7.9	2.5	"
average		248^{254}_{242}	10.8	1.4	0.652	260^{264}_{257}	8.0	0.9	260
T640c	G	243^{266}_{224}	11.0	4.1	0.718	256^{261}_{251}	7.1	1.5	260
	Y	241^{253}_{230}	10.7	2.8	0.686	269^{274}_{263}	7.1	1.4	"
	W	239^{257}_{224}	10.9	3.4	0.725	268^{274}_{262}	6.6	1.6	"
average		240^{250}_{231}	10.9	2.0	0.709	264^{267}_{261}	7.0	0.9	260

Plate Number		T(0.5) °K	$W_o(0.5)$ mÅ	σ♀ Percent	b	T(b) °K	$W_o(b)$ mÅ	σ♀ Percent	T_o °K
T641a	G	256^{271}_{242}	10.3	3.0	0.586	266^{276}_{256}	8.7	2.1	260
	Y	241^{258}_{226}	10.0	3.5	0.669	253^{261}_{246}	7.2	2.0	"
	W	249^{268}_{233}	9.9	3.7	0.657	262^{271}_{253}	7.3	2.2	"
average		249^{258}_{240}	10.0	2.0	0.647	260^{265}_{255}	7.6	1.3	260
T641b	G	249^{262}_{237}	10.6	2.7	0.601	259^{268}_{250}	8.8	2.1	260
	Y	247^{262}_{233}	10.1	3.2	0.660	260^{268}_{253}	7.5	1.9	"
	W	249^{262}_{238}	10.3	2.6	0.585	261^{270}_{253}	8.7	2.0	"
average		248^{256}_{241}	10.3	1.7	0.618	261^{266}_{256}	8.3	1.2	260
T641c	G	224^{235}_{213}	11.1	2.9	0.609	237^{245}_{230}	8.9	2.1	240
	Y	217^{230}_{206}	10.4	3.4	0.682	241^{248}_{234}	7.3	2.2	"
	W	224^{238}_{212}	10.4	3.4	0.643	245^{253}_{237}	7.9	2.3	"
average		222^{229}_{215}	10.7	1.9	0.644	241^{246}_{237}	8.0	1.4	240
T644a	G	200^{213}_{188}	11.3	4.2	0.807	244^{250}_{238}	5.9	1.9	240
	Y	212^{229}_{197}	10.8	4.6	0.737	240^{246}_{234}	6.8	1.8	"
	W	210^{226}_{195}	10.8	4.7	0.752	238^{244}_{233}	6.6	1.8	"
average		207^{216}_{199}	10.9	2.6	0.756	239^{243}_{236}	6.6	1.0	240

Plate Number		T(0.5) °K	$W_o(0.5)$ mÅ	σ♀ Percent	b	T(b) °K	$W_o(b)$ mÅ	σ♀ Percent	T_o °K
T644b	G	218^{229}_{209}	10.9	2.8	0.637	235^{242}_{228}	8.3	2.2	240
	Y	226^{239}_{214}	10.4	3.3	0.667	245^{252}_{238}	7.5	2.2	"
	W	223^{236}_{211}	10.3	3.4	0.673	244^{252}_{237}	7.4	2.3	"
average		222^{229}_{216}	10.5	1.8	0.660	242^{246}_{237}	7.6	1.3	240
T644c	G	230^{237}_{224}	11.0	1.6	0.623	249^{252}_{245}	8.5	0.9	250
	Y	236^{246}_{227}	10.4	2.2	0.669	251^{254}_{247}	7.6	1.1	"
	W	224^{234}_{215}	10.6	2.4	0.688	244^{248}_{241}	7.4	0.9	"
average		230^{235}_{225}	10.8	1.2	0.674	248^{251}_{246}	7.6	0.6	250
T645a	G	242^{250}_{233}	11.4	1.9	0.635	257^{262}_{252}	8.6	1.3	260
	Y	242^{253}_{233}	11.1	2.3	0.645	261^{267}_{256}	8.2	1.4	"
	W	236^{247}_{227}	11.0	2.5	0.666	255^{261}_{249}	7.8	1.6	"
average		240^{246}_{234}	11.1	1.3	0.646	257^{261}_{254}	8.4	0.9	260
T645b	G	223^{229}_{217}	11.5	1.6	0.531	230^{235}_{225}	10.8	1.2	230
	Y	197^{204}_{191}	11.3	2.2	0.641	227^{232}_{223}	8.4	1.4	"
	W	208^{215}_{203}	11.3	1.9	0.612	228^{232}_{223}	9.0	1.2	"
average		209^{213}_{205}	11.5	1.2	0.595	226^{229}_{223}	9.3	0.8	230

Plate Number		T(0.5) °K	$W_o(0.5)$ mÅ	$\sigma_{♀}$ Percent	b	T(b) °K	$W_o(b)$ mÅ	$\sigma_{♀}$ Percent	T_o °K
T645c	G	252_{242}^{263}	11.1	2.2	0.555	255_{248}^{262}	10.0	1.7	240
	Y	229_{219}^{239}	11.3	2.5	0.625	245_{239}^{251}	8.9	1.8	"
	W	220_{212}^{229}	11.3	2.3	0.650	240_{235}^{247}	8.3	1.7	"
average		233_{228}^{239}	11.3	1.4	0.597	245_{241}^{249}	9.3	1.0	240
T647b	G	234_{220}^{249}	9.8	3.7	0.691	256_{245}^{268}	6.7	2.9	260
	Y	235_{223}^{248}	10.6	3.1	0.687	253_{245}^{261}	7.2	2.2	"
	W	242_{228}^{258}	9.7	3.4	0.691	258_{247}^{269}	6.6	2.5	"
average		237_{229}^{246}	10.0	2.0	0.689	257_{251}^{263}	6.8	1.5	260
T647c	G	233_{225}^{242}	10.4	2.2	0.649	255_{250}^{260}	7.6	1.3	250
	Y	224_{214}^{235}	10.2	2.8	0.736	251_{247}^{256}	6.3	1.4	"
	W	216_{207}^{226}	10.2	2.7	0.684	244_{238}^{249}	7.0	1.5	"
average		224_{219}^{230}	10.3	1.5	0.691	252_{249}^{255}	6.9	0.8	250
T648a	G	238_{232}^{245}	10.8	1.4	0.578	247_{244}^{250}	9.3	0.9	250
	Y	238_{231}^{246}	10.5	1.7	0.622	253_{249}^{257}	8.2	1.1	"
	W	238_{230}^{247}	10.3	2.0	0.635	252_{249}^{256}	7.9	1.0	"
average		238_{234}^{243}	10.5	1.0	0.603	250_{247}^{252}	8.7	0.7	250

Plate Number		T(0.5) °K	W_o(0.5) mÅ	σ♀ Percent	b	T(b) °K	W_o(b) mÅ	σ♀ Percent	T_o °K
T648b	G	242^{251}_{233}	10.3	2.0	0.640	253^{257}_{249}	7.8	1.0	250
	Y	233^{242}_{224}	10.1	2.2	0.664	248^{251}_{246}	7.4	0.7	"
	W	222^{232}_{214}	10.4	2.4	0.695	241^{244}_{238}	7.1	0.9	"
average		232^{237}_{227}	10.3	1.3	0.668	248^{250}_{246}	7.4	0.5	250
T649b	G	218^{235}_{203}	10.8	4.4	0.735	241^{246}_{236}	6.9	1.7	240
	Y	209^{228}_{193}	10.1	5.2	0.832	234^{239}_{229}	5.4	1.9	"
	W	203^{216}_{191}	10.5	4.1	0.789	236^{242}_{230}	5.9	2.2	"
average		210^{219}_{201}	10.5	2.7	0.778	237^{240}_{233}	6.1	1.2	240
T650b	G	232^{242}_{223}	11.0	2.3	0.669	248^{252}_{244}	8.1	1.3	250
	Y	229^{236}_{223}	11.5	1.7	0.648	249^{252}_{245}	8.5	1.1	"
	W	226^{235}_{218}	11.2	2.3	0.680	244^{247}_{241}	7.9	1.0	"
average		229^{234}_{225}	11.3	1.2	0.669	247^{250}_{245}	8.1	0.6	250
T650c	G	244^{253}_{235}	11.8	2.0	0.668	251^{256}_{246}	8.5	1.2	250
	Y	228^{237}_{220}	11.5	2.2	0.707	247^{251}_{242}	7.5	1.1	"
	W	236^{246}_{227}	11.4	2.3	0.725	246^{251}_{242}	7.3	1.2	"
average		236^{241}_{231}	11.5	1.3	0.687	249^{252}_{246}	8.0	0.7	250

Plate Number		T(0.5) °K	$W_o(0.5)$ mÅ	$\sigma_♀$ Percent	b	T(b) °K	$W_o(b)$ mÅ	$\sigma_♀$ Percent	T_o °K
T651a	G	234^{249}_{220}	11.5	3.7	0.707	259^{264}_{254}	7.6	1.3	260
	Y	238^{255}_{224}	11.1	3.6	0.780	269^{274}_{264}	6.2	1.3	"
	W	236^{252}_{231}	11.1	3.7	0.754	261^{266}_{255}	6.7	1.6	"
average		236^{245}_{228}	11.2	2.1	0.749	262^{264}_{259}	6.9	0.9	260
T651b	G	232^{242}_{222}	11.7	2.5	0.640	247^{253}_{242}	8.9	1.6	250
	Y	229^{239}_{221}	11.5	2.2	0.653	253^{257}_{248}	8.3	1.4	"
	W	237^{248}_{226}	11.5	2.6	0.665	258^{264}_{253}	8.0	1.5	"
average		233^{238}_{227}	11.5	1.4	0.649	251^{255}_{248}	8.5	0.9	250
T651c	G	237^{246}_{228}	11.4	2.2	0.542	244^{251}_{237}	10.4	1.7	240
	Y	235^{245}_{226}	11.3	2.3	0.583	245^{252}_{238}	9.5	1.7	"
	W	233^{243}_{224}	11.4	2.3	0.579	242^{249}_{236}	9.6	1.8	"
average		235^{240}_{230}	11.4	1.3	0.566	244^{248}_{240}	9.9	1.0	240
T654b	G	238^{251}_{227}	9.8	2.7	0.651	255^{262}_{249}	7.2	1.8	260
	Y	238^{252}_{226}	9.9	3.1	0.729	263^{269}_{257}	6.2	1.5	"
	W	234^{248}_{221}	9.8	3.3	0.690	252^{258}_{246}	6.7	1.7	"
average		237^{244}_{230}	9.8	1.7	0.692	258^{262}_{255}	6.7	1.0	260

Plate Number		T(0.5) °K	$W_o(0.5)$ mÅ	σ_o Percent	b	T(b) °K	$W_o(b)$ mÅ	σ ♀ Percent	T_o °K
T655b	G	215^{226}_{206}	10.6	2.8	0.705	238^{243}_{233}	7.0	1.5	240
	Y	229^{239}_{220}	10.4	2.5	0.629	244^{250}_{238}	8.1	1.7	"
	W	233^{245}_{223}	10.2	2.7	0.622	248^{255}_{241}	8.0	1.9	"
average		226^{232}_{220}	10.3	1.5	0.648	244^{247}_{240}	7.7	1.0	240
T657b	G	235^{245}_{225}	10.7	2.5	0.688	250^{253}_{246}	7.5	1.1	250
	Y	231^{242}_{221}	10.6	2.6	0.709	251^{255}_{247}	7.0	1.1	"
	W	226^{236}_{217}	10.7	2.5	0.702	241^{244}_{238}	7.3	1.0	"
average		230^{236}_{225}	10.7	1.4	0.695	247^{249}_{245}	7.4	0.6	250
T658b	G	235^{246}_{224}	11.3	2.5	0.684	257^{263}_{252}	7.8	1.4	260
	Y	237^{250}_{225}	11.1	2.9	0.712	260^{266}_{254}	7.2	1.7	"
	W	232^{243}_{220}	11.1	2.6	0.705	256^{262}_{251}	7.2	1.6	"
average		234^{241}_{228}	11.1	1.5	0.702	257^{260}_{254}	7.4	0.9	260
T660b	G	226^{236}_{217}	10.8	2.4	0.694	255^{261}_{249}	7.2	1.5	250
	Y	217^{226}_{209}	10.9	2.3	0.694	248^{252}_{243}	7.3	1.2	"
	W	222^{230}_{214}	10.8	2.1	0.705	249^{253}_{246}	7.1	1.0	"
average		222^{227}_{217}	10.9	1.3	0.699	251^{253}_{248}	7.2	0.7	250

Plate Number		T(0.5) °K	$W_o(0.5)$ mÅ	σ ♀ Percent	b	T(b) °K	$W_o(b)$ mÅ	σ ♀ Percent	T_o °K
T660c	G	257^{267}_{248}	9.8	2.0	0.488	257^{266}_{249}	10.0	1.7	250
	Y	235^{244}_{227}	9.7	2.0	0.610	248^{253}_{243}	7.8	1.3	"
	W	234^{243}_{226}	9.7	2.1	0.575	242^{248}_{237}	8.2	1.6	"
	G	226^{233}_{218}	10.6	1.9	0.526	231^{237}_{225}	10.0	1.6	"
	Y	235^{243}_{227}	9.7	1.9	0.577	241^{246}_{236}	8.4	1.4	"
	W	238^{249}_{229}	9.3	2.3	0.622	248^{254}_{242}	7.4	1.5	"
average		237^{241}_{233}	9.8	0.9	0.574	245^{248}_{242}	8.4	0.7	250
T661b	G	244^{262}_{228}	10.5	3.9	0.704	265^{274}_{258}	6.9	2.1	260
	Y	238^{256}_{223}	10.3	3.9	0.711	260^{267}_{254}	6.8	1.9	"
	W	241^{259}_{226}	10.5	3.9	0.720	262^{269}_{256}	6.7	1.8	"
average		241^{251}_{232}	10.5	2.2	0.713	262^{266}_{258}	6.8	1.1	260
T661c	G	227^{234}_{220}	11.6	1.8	0.679	249^{252}_{246}	8.1	0.9	250
	Y	228^{236}_{221}	11.5	2.0	0.688	249^{253}_{246}	7.8	1.1	"
	W	218^{226}_{210}	11.5	2.2	0.694	243^{247}_{239}	7.7	1.2	"
average		224^{229}_{220}	11.5	1.2	0.685	248^{250}_{246}	7.8	0.6	250

Table 4
Temperatures found for different values of T_o.

	Measurer of Plate T660B								
	G	Y	W	G	Y	W	G	Y	W
T_o, °K	T(b), °K			Standard deviation			ΔT, °K		
240	254	247	248	.0697	.0561	.0489	+14	+7	+8
250	255	248	249	.0663	.0540	.0465	+ 5	−2	−1
260	260	251	253	.0663	.0570	.0477	+0	−9	−7

Table 5
Summary of Table 3

Plate Number	Slit Position	Square Root Absorption Law: T(0.5) °K	Square Root Absorption Law: $W_o(0.5)$ mÅ	Square Root Absorption Law: $\sigma_{♀}$ Percent	Curve of Growth Absorption Law: b	Curve of Growth Absorption Law: T(b) °K	Curve of Growth Absorption Law: $W_o(b)$ mÅ	Curve of Growth Absorption Law: $\sigma_{♀}$ Percent
T622	Std	214^{219}_{210}	11.3	1.2	0.677	236^{238}_{233}	8.0	0.9
T624a	T	222^{228}_{216}	11.8	1.5	0.606	241^{245}_{236}	9.5	1.2
T624b	L	209^{219}_{201}	11.0	2.8	0.779	238^{242}_{234}	6.5	1.5
T625a	Std	243^{252}_{234}	11.1	2.1	0.714	263^{267}_{259}	7.2	1.0
T625b	S −28	227^{235}_{220}	11.5	2.0	0.655	243^{247}_{239}	8.5	1.2
T625c	N +27	222^{229}_{216}	12.0	1.8	0.678	239^{243}_{236}	8.6	1.0
T627a	Std	219^{225}_{213}	10.8	1.6	0.703	235^{237}_{232}	7.4	0.8
T630a	Std+18°	227^{235}_{219}	10.5	2.1	0.678	243^{246}_{239}	7.5	1.1
T630b	N +26	238^{250}_{227}	9.8	2.7	0.780	266^{272}_{261}	5.7	1.5
T630c	NN +54	226^{232}_{220}	12.5	1.6	0.551	248^{254}_{243}	11.2	1.2
T631a	Eq −9	227^{234}_{221}	10.3	1.7	0.733	260^{263}_{256}	6.4	1.0
T631b	S −17	241^{248}_{235}	10.7	1.5	0.535	243^{248}_{238}	10.2	1.2
T633a	Std+30	228^{234}_{223}	11.2	1.4	0.658	245^{248}_{242}	8.3	0.8
T633b	Eq −6	225^{229}_{222}	11.0	1.0	0.661	248^{250}_{246}	8.0	0.6
T636a	Std+28	238^{245}_{232}	10.5	1.6	0.704	264^{267}_{260}	6.9	0.9
T636b	S −24	229^{234}_{224}	10.7	1.2	0.682	250^{258}_{248}	7.3	0.8
T636c	N +15	222^{227}_{218}	10.5	1.3	0.714	248^{250}_{245}	6.9	0.7

Plate Number	Slit Position	T(0.5) °K	Wo(0.5) mÅ	$\sigma_{♀}$ Percent	b	T(b) °K	Wo(b) mÅ	$\sigma_{♀}$ Percent
T640a	Std+19	223^{235}_{212}	11.7	1.6	0.659	239^{242}_{236}	8.8	0.8
T640b	Eq -2	248^{254}_{242}	10.8	1.4	0.652	260^{264}_{257}	8.0	0.9
T640c	S -33	240^{250}_{231}	10.9	2.0	0.709	264^{267}_{261}	7.0	0.9
T641a	Eq +8	249^{258}_{240}	10.0	2.0	0.647	260^{265}_{255}	7.6	1.3
T641b	Eq +10	248^{256}_{241}	10.3	1.7	0.618	261^{266}_{256}	8.3	1.2
T641c	L +50	222^{229}_{215}	10.7	1.9	0.644	241^{246}_{237}	8.0	1.4
T644a	Std+24	207^{216}_{199}	10.9	2.6	0.756	239^{243}_{236}	6.6	1.0
T644b	L +47	222^{229}_{216}	10.5	1.8	0.660	242^{246}_{237}	7.6	1.3
T644c	T +0	230^{235}_{225}	10.8	1.2	0.674	248^{251}_{246}	7.6	0.6
T645a	Eq -6	240^{246}_{234}	11.1	1.3	0.646	257^{261}_{254}	8.4	0.9
T645b	N +42	209^{213}_{205}	11.5	1.2	0.595	226^{229}_{223}	9.3	0.8
T645c	S -36	233^{239}_{228}	11.3	1.4	0.597	245^{249}_{241}	9.3	1.0
T647b	N +42	237^{246}_{229}	10.0	2.0	0.689	257^{263}_{251}	6.8	1.5
T647c	Eq -4	224^{230}_{219}	10.3	1.5	0.691	252^{255}_{249}	6.9	0.8
T648a	S -28	238^{243}_{234}	10.5	1.0	0.603	250^{252}_{247}	8.7	0.7
T648b	Std+21	232^{237}_{227}	10.3	1.3	0.668	248^{250}_{246}	7.4	0.5
T649b	Std	210^{219}_{201}	10.5	2.7	0.778	237^{240}_{233}	6.1	1.2

Plate Number	Slit Position	T(0.5) °K		$W_o(0.5)$ mÅ	$\sigma_{♀}$ Percent	b	T(b)		Wo(b)	$\sigma_{♀}$
T650b	Std+17	229^{234}_{225}		11.3	1.2	0.669	247^{250}_{245}		8.1	0.6
T650c	Eq -6	236^{241}_{231}		11.5	1.3	0.687	249^{252}_{246}		8.0	0.7
T651a	N +32	236^{252}_{231}		11.2	2.1	0.749	262^{264}_{259}		6.9	0.9
T651b	S -37	233^{238}_{227}		11.5	1.4	0.649	251^{255}_{248}		8.5	0.9
T651c	Std+37	235^{240}_{230}		11.4	1.3	0.566	244^{248}_{240}		9.9	1.0
T654b	Std+12	237^{244}_{230}		9.8	1.7	0.692	258^{262}_{255}		6.7	1.0
T655b	Std+13	226^{232}_{220}		10.3	1.5	0.648	244^{247}_{240}		7.7	1.0
T657b	Std+15	230^{236}_{225}		10.7	1.4	0.695	247^{249}_{245}		7.4	0.6
T658b	Std+15	234^{241}_{228}		11.1	1.5	0.702	257^{260}_{254}		7.4	0.9
T660b	Std+12	222^{227}_{217}		10.9	1.3	0.699	251^{253}_{248}		7.2	0.7
T660c	Eq +10	237^{241}_{233}		9.8	0.9	0.574	245^{248}_{242}		8.4	0.7
T661b	Std	241^{251}_{232}		10.5	2.2	0.713	262^{266}_{258}		6.8	1.1
T661c	Eq +0	224^{229}_{220}		11.5	1.2	0.685	248^{250}_{246}		7.8	0.6
		σ_{int}	σ_{ext}				σ_{int}	σ_{ext}		
average	Eq	236±2.2	3.3	10.7	0.5	0.659	254±1.3	2.6	7.7	0.3
average	N	227±3.2	4.0	11.1	0.8	0.679	249±1.8	5.2	7.9	0.5
average	S	234±2.6	2.1	11.0	0.6	0.633	249±1.5	2.8	8.5	0.4
average	L	218±5.4	4.3	10.7	1.6	0.694	240±3.1	1.2	7.5	1.0
average	T	226±5.5	4.0	11.3	1.4	0.640	245±3.6	3.5	8.6	0.9
average	Std	228±1.6	2.2	10.8	0.4	0.688	248±0.8	2.1	7.5	0.2
average	all	230±1.3	1.5	10.9	0.25	0.671	249±0.6	1.4	7.8	0.15

Table 6

Summary of Measurements of Temperatures over different areas of Venus .

Band head, Å	reference	Slit Alignment parallel to equator T(°K)	n	pole-to-pole T(°K)	n	ΔT °K
7820	Present results	251±2	(24)	247±2	(23)	4±3
7820	Young et al, 1971	250±4	(4)	240±2	(11)	10±5
7820	Schorn et al, 1969	253±4	(7)	246±3	(11)	7±5
8689	Schorn et al, 1974	242±2	(7)	248±2	(23)	-6±3
8689	Young et al. 1969	239±3	(15)	236±4	(15)	3±5
10488	Young et al, 1970	238±3	(6)	237±3	(25)	1±4
10627	Schorn et al, 1971	274±15	(6)	234±3	(25)	40±15
10362	Schorn et al, 1970	------		237±3	(15)	---
12030 12177	Young et al. 1970	------		236±5	(10)	---

Table 7
Variation in temperature and CO_2
Abundance from the average
value for Each region on Venus

Plate Number	Slit Position	Date 1972	$W_o(0.5)$ $m\mathring{A}$	$T(b)$ ^oK
T622	Std	IX 17.556	+0.5	-12
T624a	T	IX 17.731	+0.5	- 4
T625a	Std	IX 18.549	+0.3	+15
T625b	S	IX 18.598	+0.5	- 6
T625c	N	IX 18.620	+0.9	-10
T627a	Std	IX 19.634	0.0	- 7
T630a	Std	IX 20.629	-0.3	- 5
T630b	N	IX 20.653	-1.3	+17
T630c	NN	IX 20.677	+1.4	- 1
T631a	Eq	IX 20.722	-0.4	+ 6
T631b	S	IX 20.759	-0.3	- 6
T633a	Std	IX 21.630	+0.4	- 3
T633b	Eq	IX 21.667	+0.3	- 6
T636a	Std	IX 23.615	+0.9	+16
T636b	S	IX 23.654	-0.3	+ 1
T636c	N	IX 23.692	-0.6	- 1
T640a	Std	IX 25.615	+0.9	- 9
T640b	Eq	IX 25.640	+0.1	+11
T640c	S	IX 25.663	-0.1	+15
T641a	Eq	IX 25.701	-0.7	+11
T641b	Eq	IX 25.738	-0.4	+12
T641c	L	IX 25.770	0.0	+ 1
T644a	Std	IX 26.614	+0.1	- 9
T644b	L	IX 26.647	-0.2	+ 2
T644c	T	IX 26.691	0.0	+ 3
T645a	Eq	IX 26.747	+0.4	+ 3
T645b	N	IX 26.780	+0.4	-23
T645c	S	IX 26.803	+0.3	- 4
T647b	N	IX 27.636	-1.1	+ 8
T647c	Eq	IX 27.659	-0.4	- 2
T648a	S	IX 27.684	-0.5	+ 1
T648b	Std	IX 27.708	-0.5	0
T649b	Std	IX 28.778	-0.3	- 9
T650b	Std	IX 30.562	+0.5	- 1
T650c	Eq	IX 30.586	+0.8	- 5
T651a	N	IX 30.616	+0.1	+13
T651b	S	IX 30.639	+0.5	+ 2
T651c	Std	IX 30.662	+0.6	- 4
T654b	Std	X 1.714	-1.0	+10
T655b	Std	X 2.565	-0.5	- 4
T657b	Std	X 3.608	-0.1	- 1
T658b	Std	X 4.575	+0.3	+ 9
T660b	Std	X 5.550	+0.1	+ 3
T660c	Eq	X 5.575	-0.8	- 9
T661b	Std	X 7.609	-0.3	+14
T661c	Eq	X 7.637	+0.8	- 6

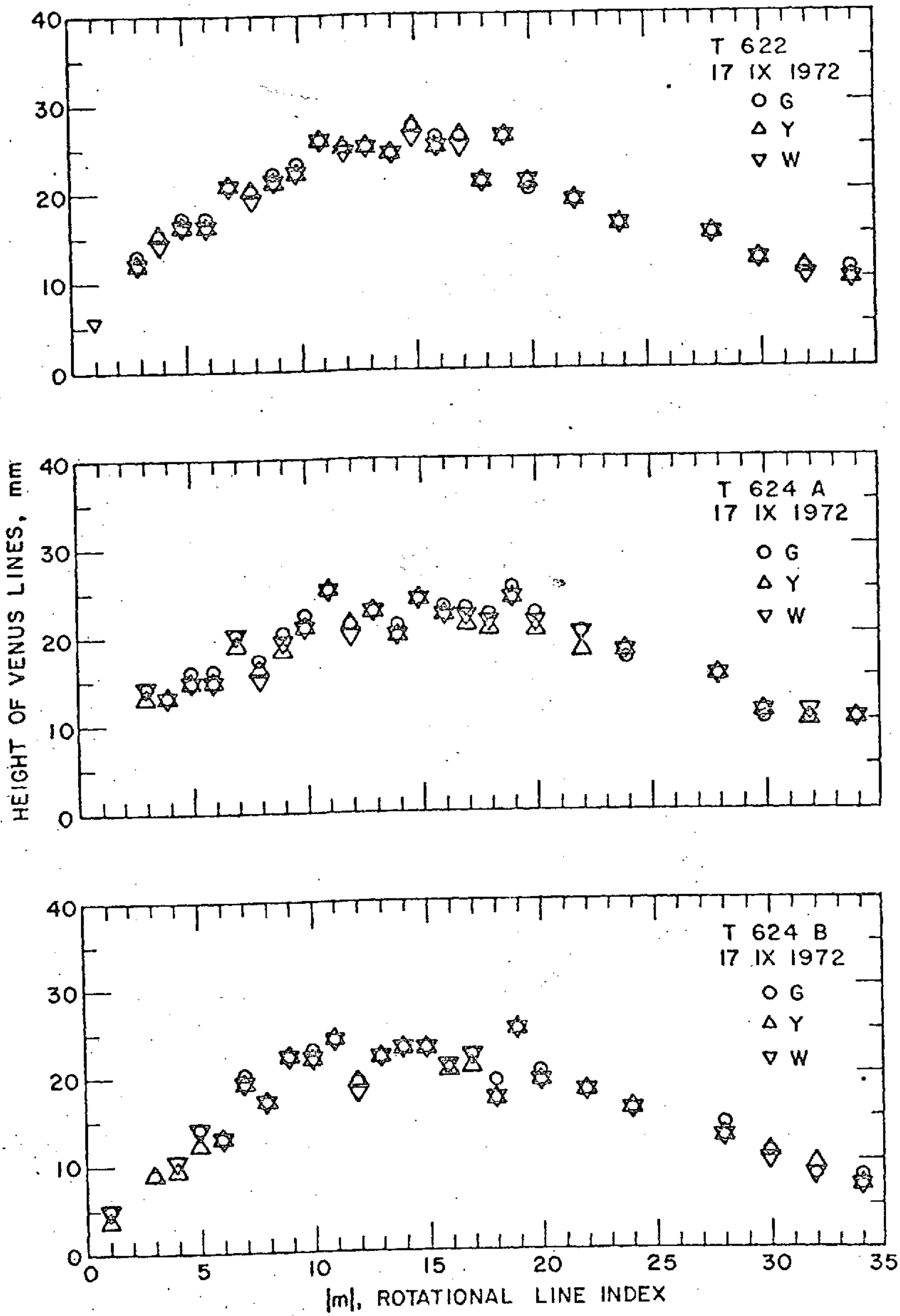

T 622
17 IX 1972
O G
Δ Y
∇ W
T 624 A
17 IX 1972
O G
Δ Y
∇ W
T 624 B
17 IX 1972
O G
Δ Y
∇ W
HEIGHT OF VENUS LINES, mm
|m|, ROTATIONAL LINE INDEX

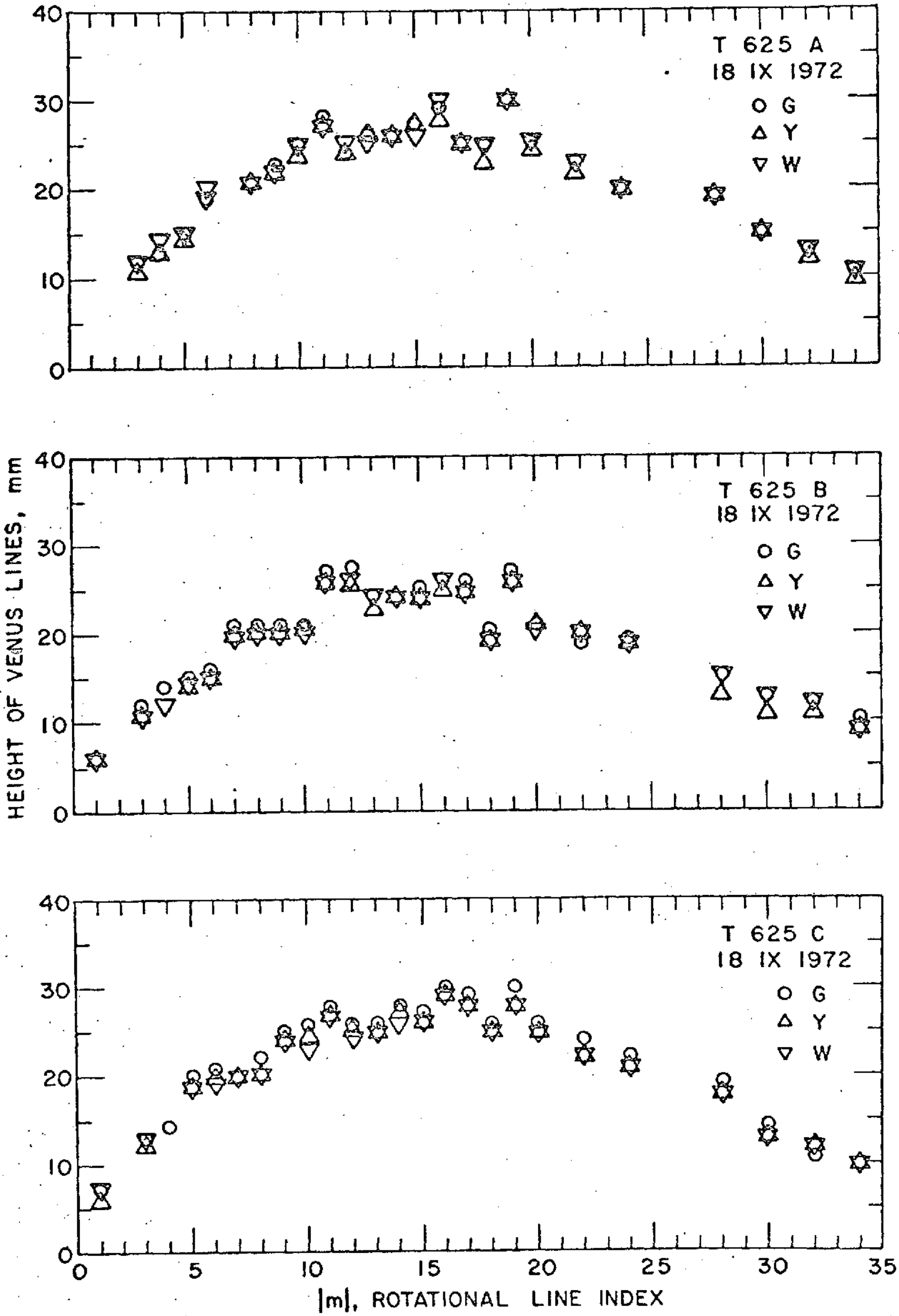

T 625 A
18 IX 1972
O G
Δ Y
∇ W
T 625 B
18 IX 1972
O G
Δ Y
∇ W
T 625 C
18 IX 1972
O G
Δ Y
∇ W
HEIGHT OF VENUS LINES, mm
0
10
20
30
40
0
5
10
15
20
25
30
35
|m|, ROTATIONAL LINE INDEX

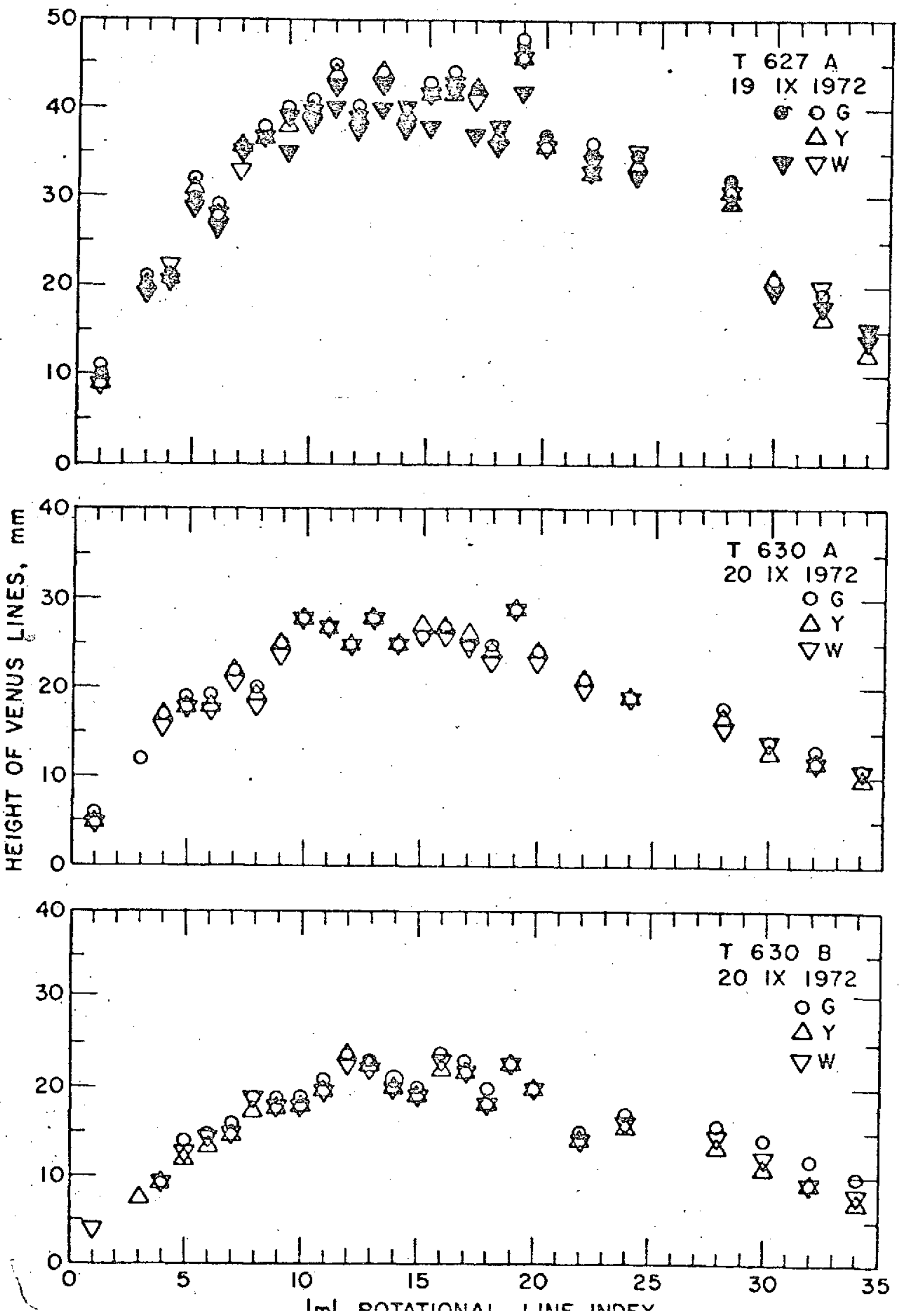

T 627 A
19 IX 1972
G
Y
W
T 630 A
20 IX 1972
G
Y
W
T 630 B
20 IX 1972
G
Y
W
HEIGHT OF VENUS LINES, mm
|m| ROTATIONAL LINE INDEX

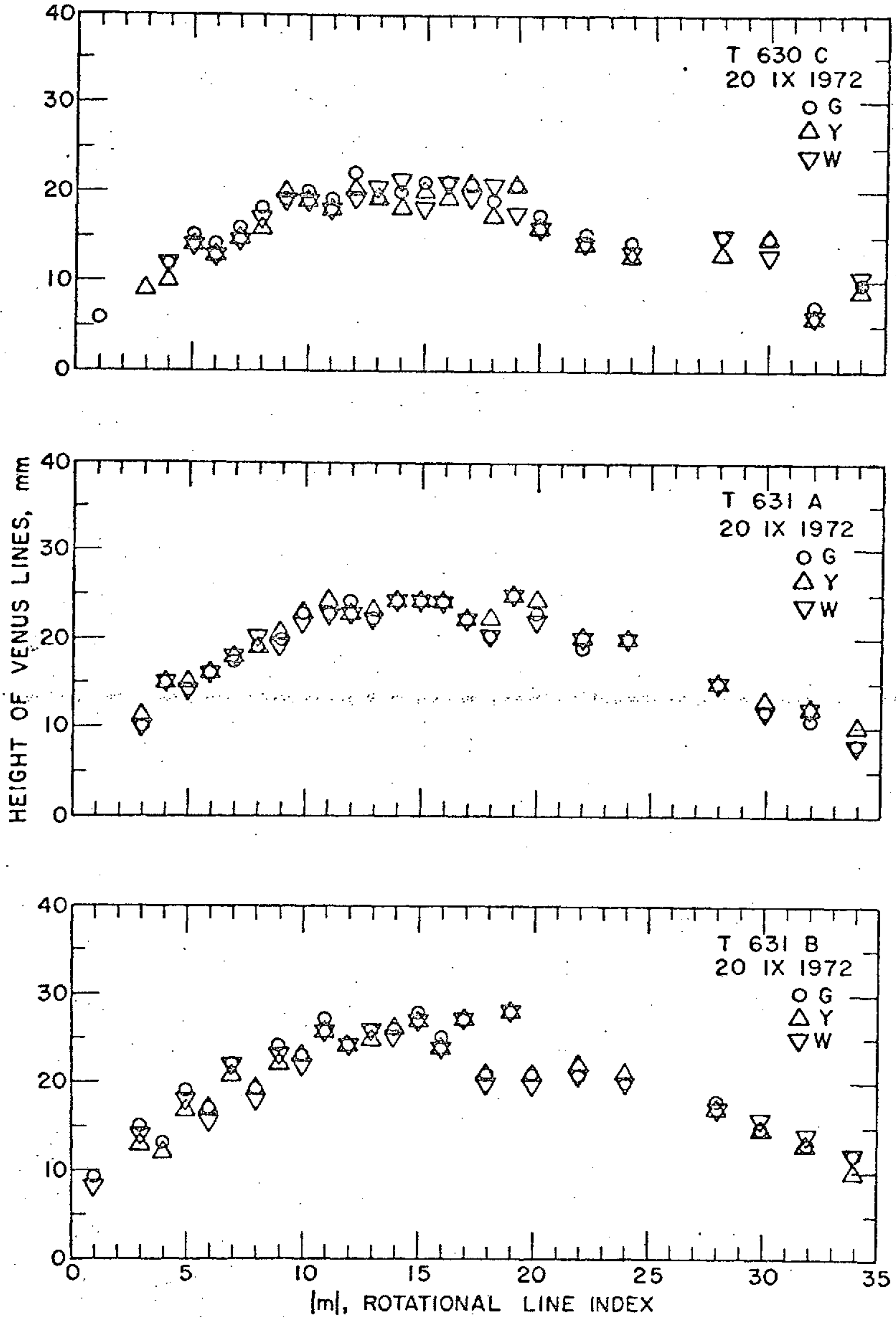
T 630 C
20 IX 1972
O G
△ Y
▽ W
T 631 A
20 IX 1972
O G
△ Y
▽ W
T 631 B
20 IX 1972
O G
△ Y
▽ W
HEIGHT OF VENUS LINES, mm
|m|, ROTATIONAL LINE INDEX
0
5
10
15
20
25
30
35
40

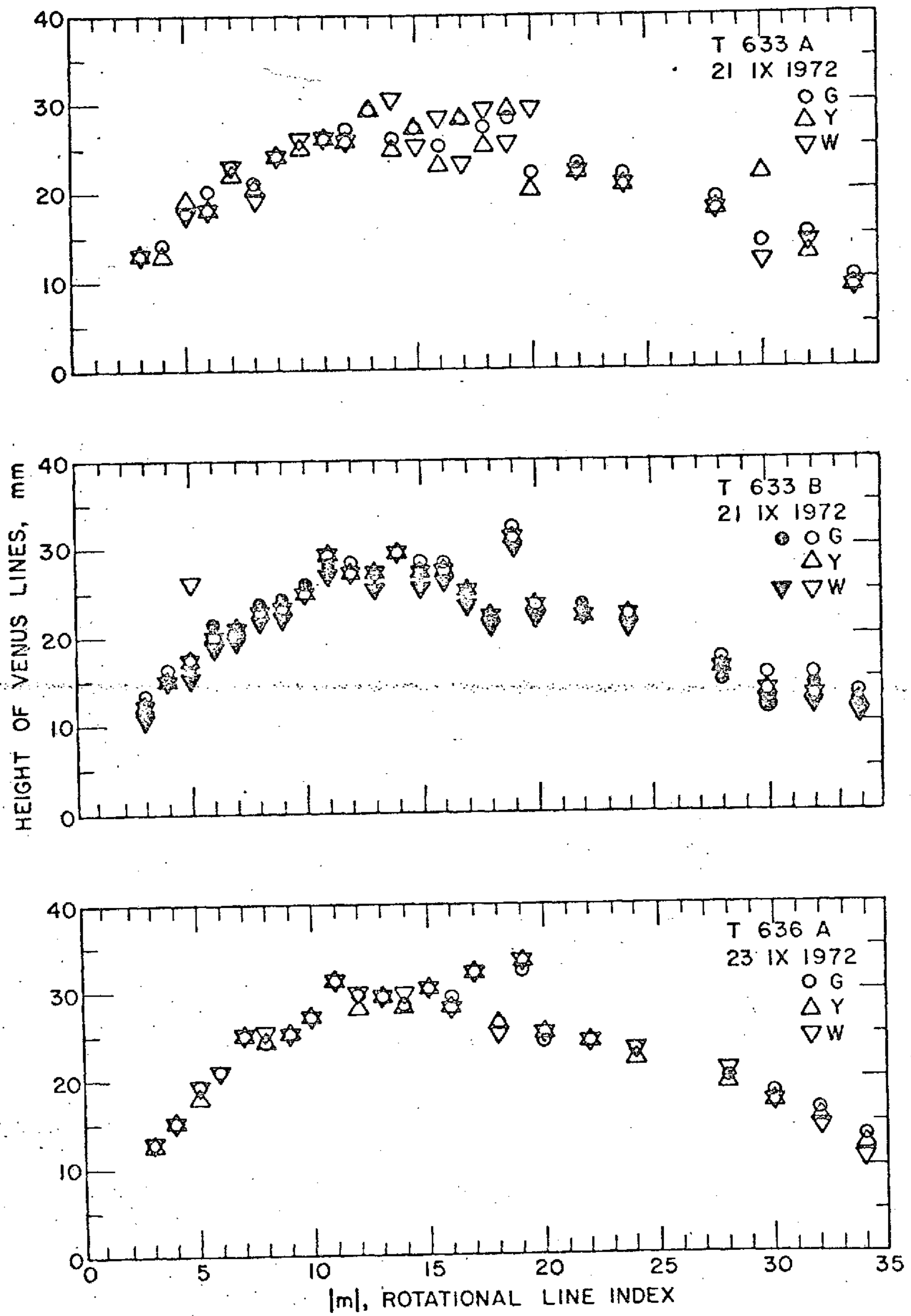

T 633 A
21 IX 1972
G
Y
W
T 633 B
21 IX 1972
G
Y
W
T 636 A
23 IX 1972
G
Y
W
HEIGHT OF VENUS LINES, mm
|m|, ROTATIONAL LINE INDEX

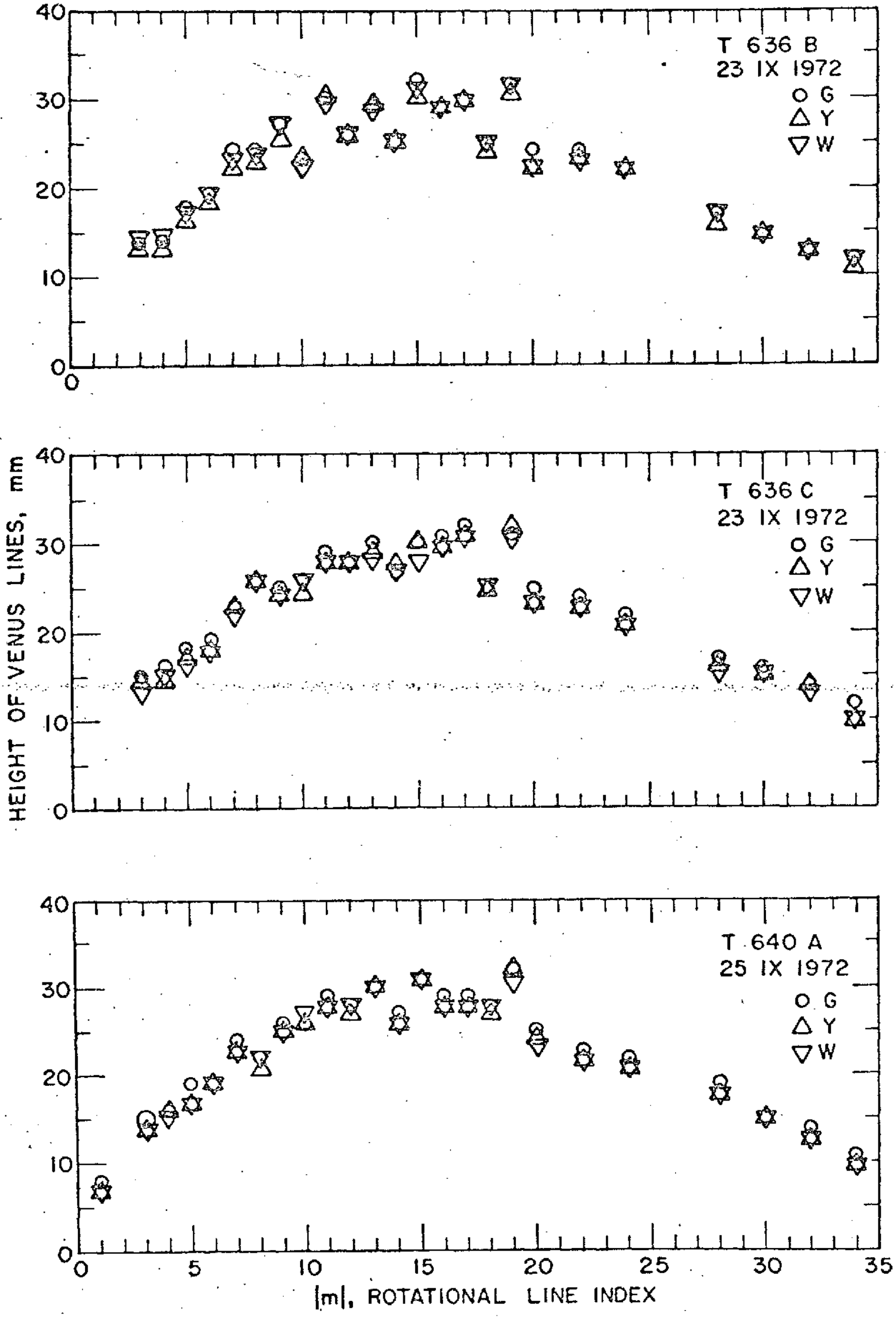
T 636 B
23 IX 1972
O G
△ Y
▽ W
T 636 C
23 IX 1972
O G
△ Y
▽ W
T 640 A
25 IX 1972
O G
△ Y
▽ W
HEIGHT OF VENUS LINES, mm
|m|, ROTATIONAL LINE INDEX
0
5
10
15
20
25
30
35
40

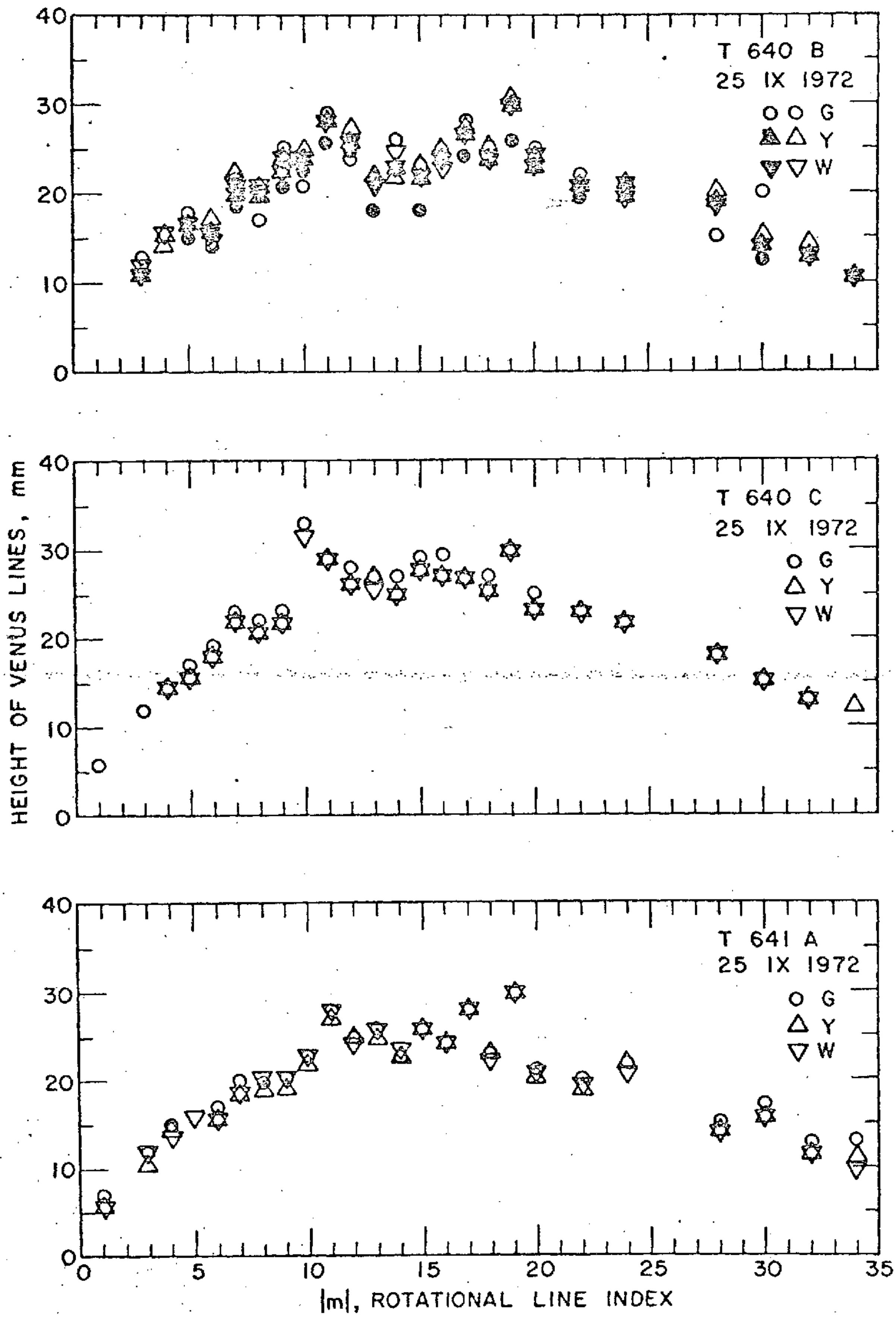

T 640 B
25 IX 1972
G
Y
W
T 640 C
25 IX 1972
G
Y
W
T 641 A
25 IX 1972
G
Y
W
HEIGHT OF VENUS LINES, mm
|m|, ROTATIONAL LINE INDEX

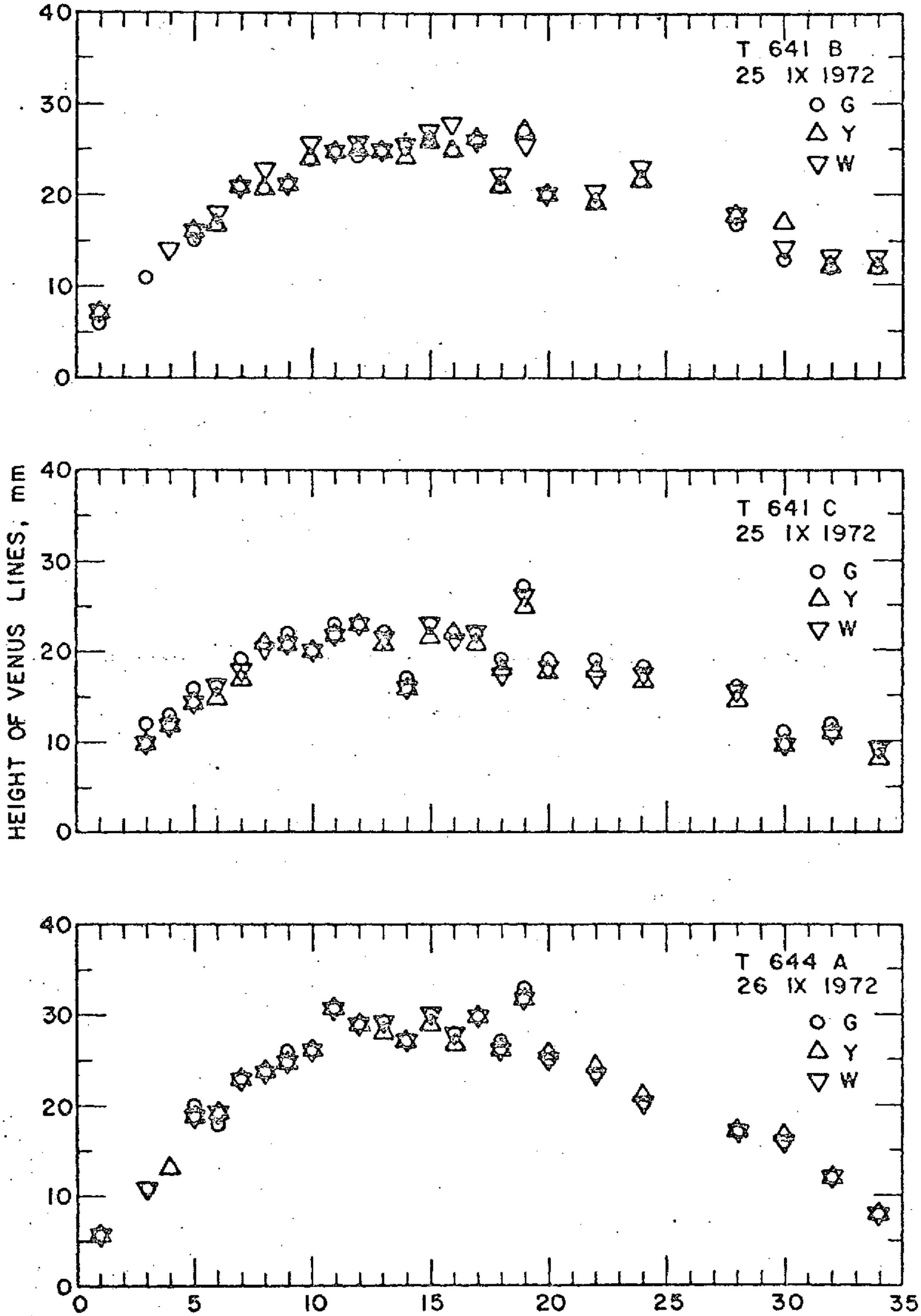
T 641 B
25 IX 1972
O G
Δ Y
∇ W
T 641 C
25 IX 1972
O G
Δ Y
∇ W
T 644 A
26 IX 1972
O G
Δ Y
∇ W
HEIGHT OF VENUS LINES, mm
0
10
20
30
40
0
5
10
15
20
25
30
35

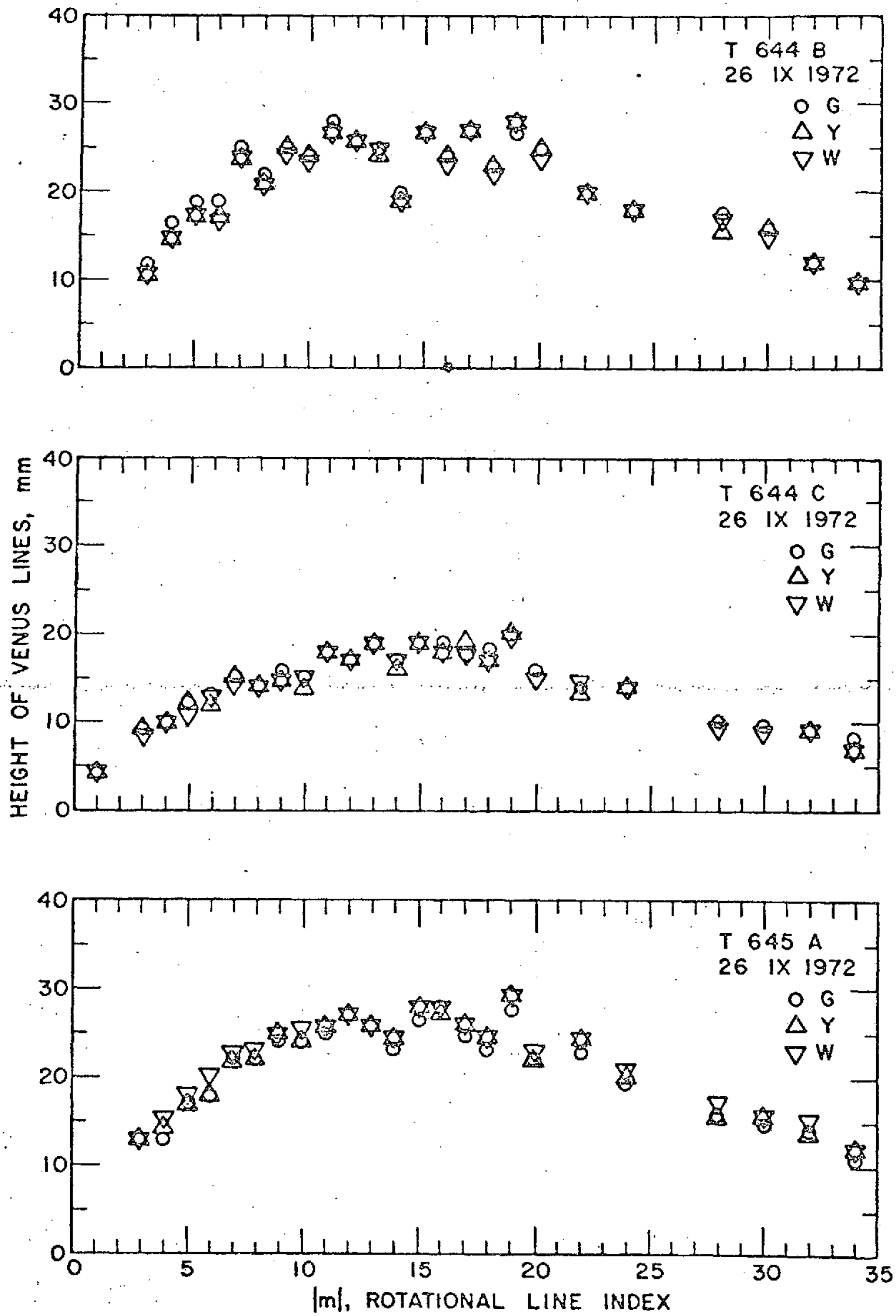

T 644 B
26 IX 1972
O G
Δ Y
▽ W
T 644 C
26 IX 1972
O G
Δ Y
▽ W
T 645 A
26 IX 1972
O G
Δ Y
▽ W
HEIGHT OF VENUS LINES, mm
|m|, ROTATIONAL LINE INDEX
0
5
10
15
20
25
30
35
40

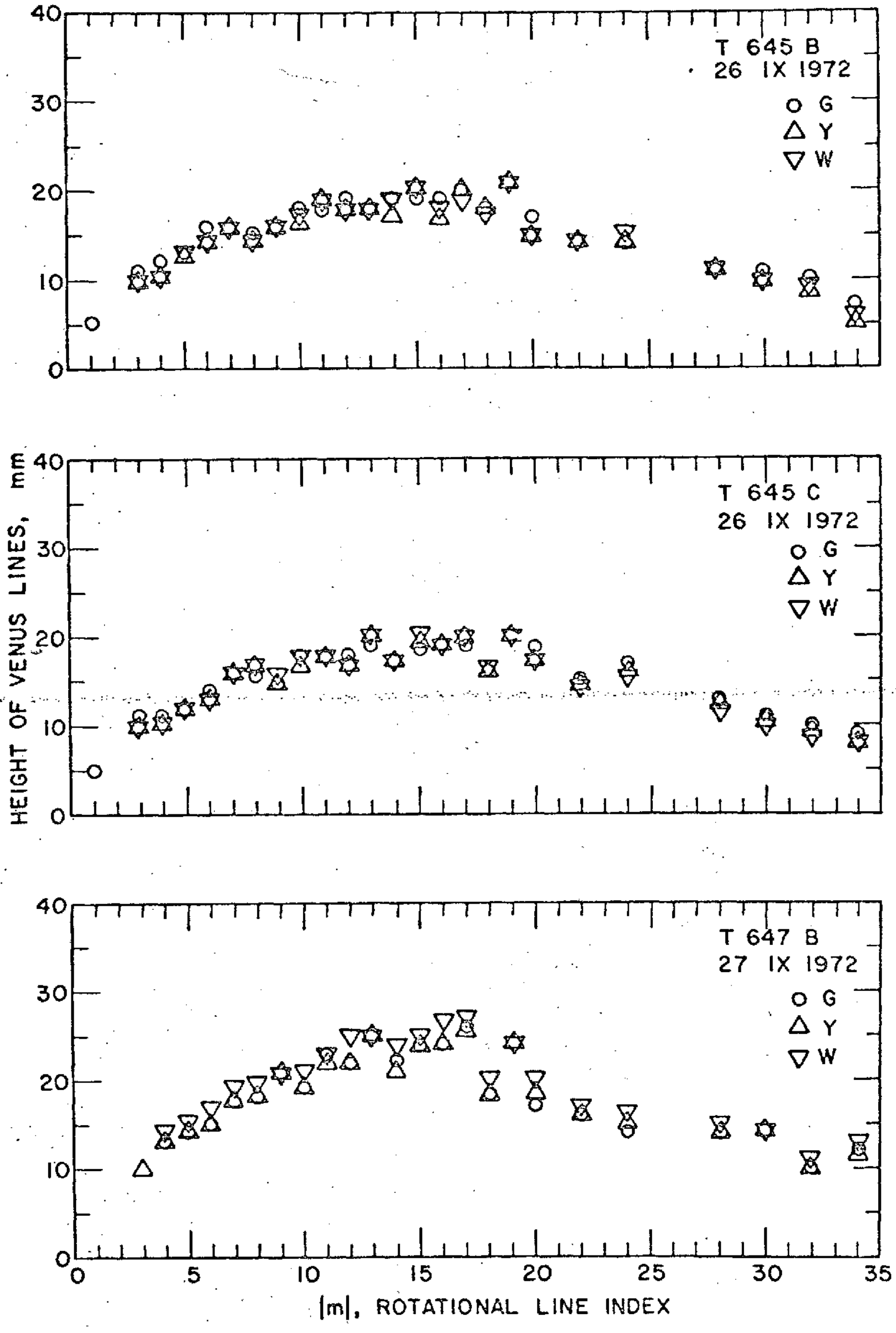
T 645 B
26 IX 1972
O G
Δ Y
∇ W
T 645 C
26 IX 1972
O G
Δ Y
∇ W
T 647 B
27 IX 1972
O G
Δ Y
∇ W
HEIGHT OF VENUS LINES, mm
|m|, ROTATIONAL LINE INDEX

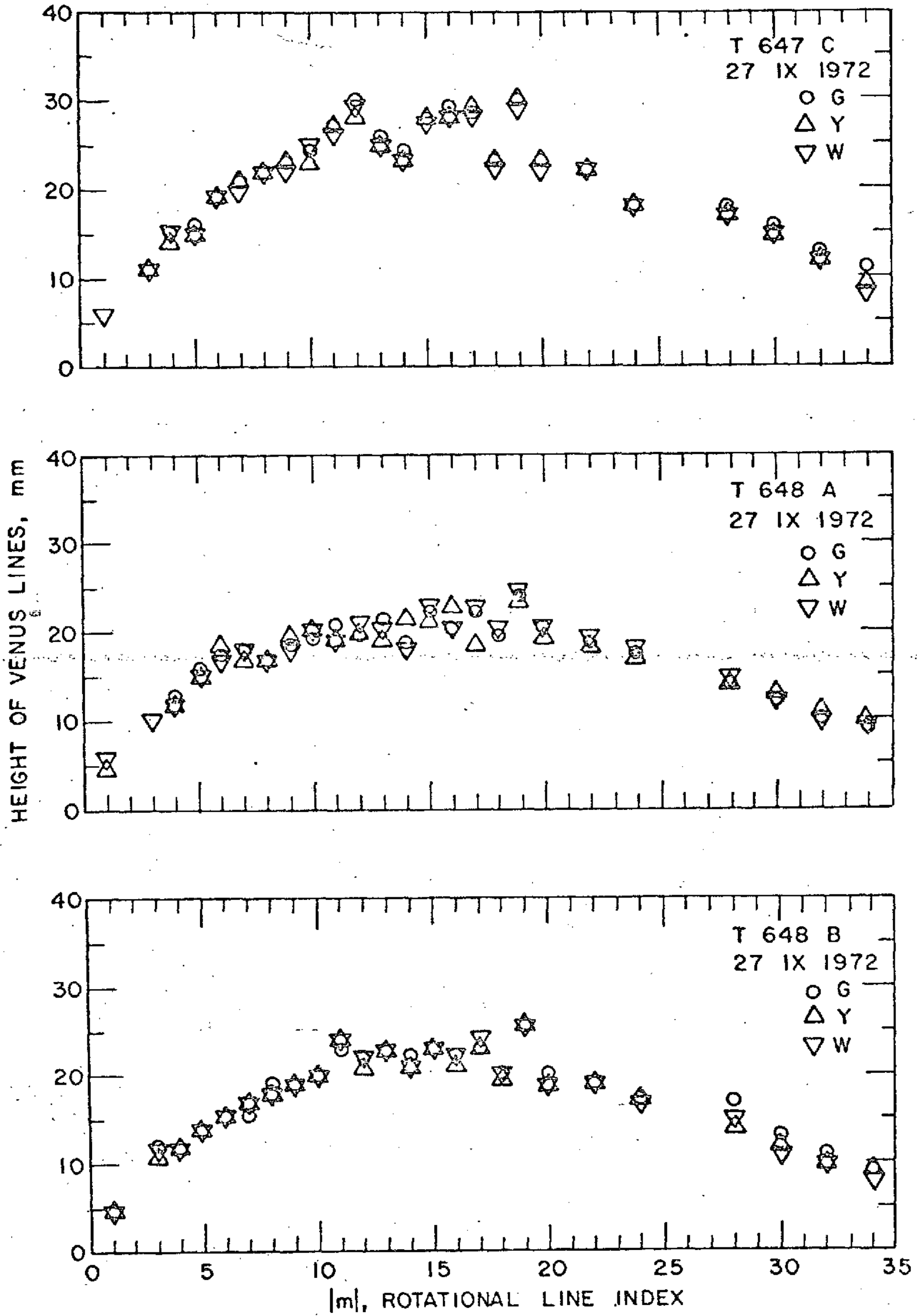
T 647 C
27 IX 1972
O G
△ Y
▽ W
T 648 A
27 IX 1972
O G
△ Y
▽ W
T 648 B
27 IX 1972
O G
△ Y
▽ W
HEIGHT OF VENUS LINES, mm
|m|, ROTATIONAL LINE INDEX
0
5
10
15
20
25
30
35
40

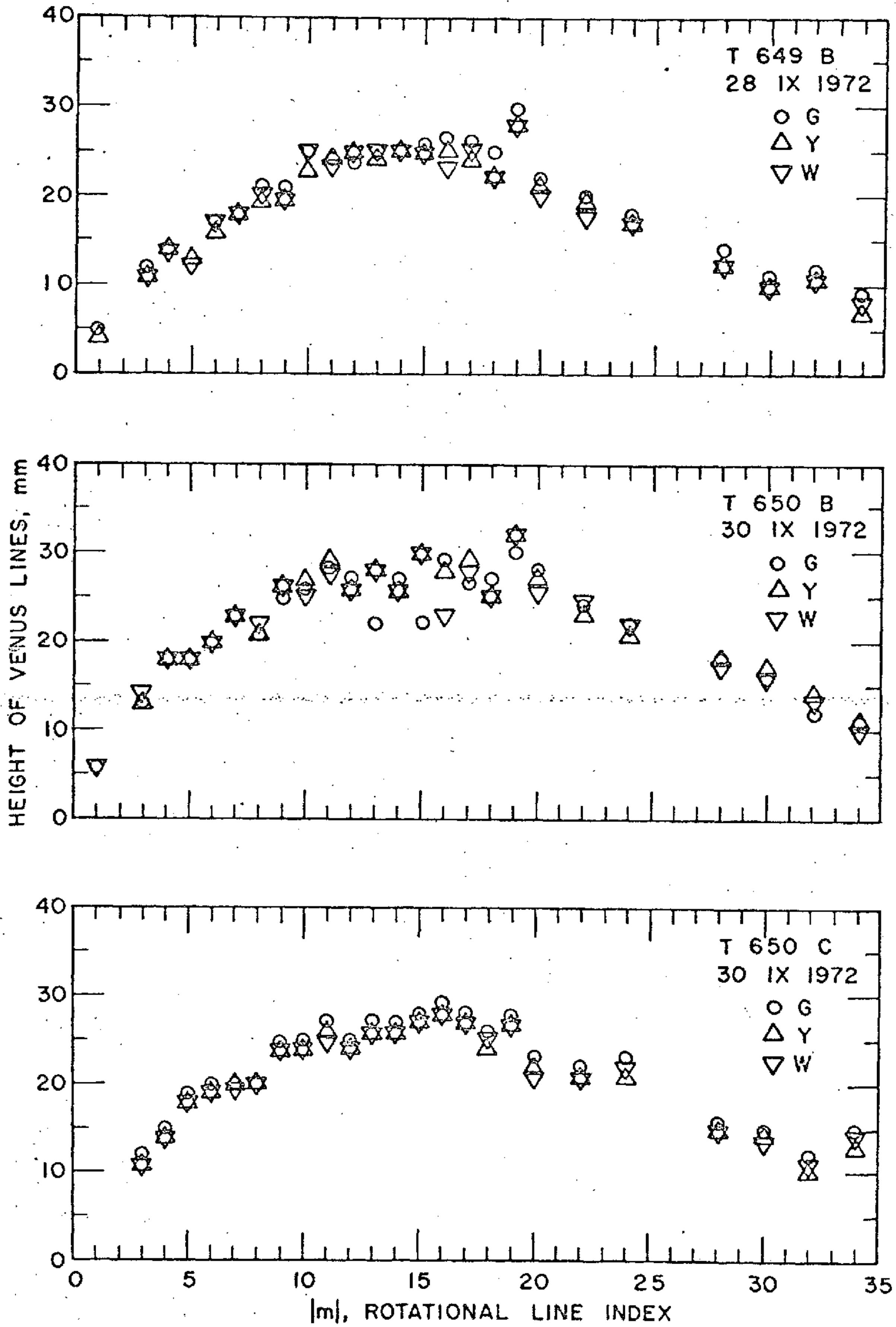

T 649 B
28 IX 1972
O G
△ Y
▽ W
T 650 B
30 IX 1972
O G
△ Y
▽ W
T 650 C
30 IX 1972
O G
△ Y
▽ W
HEIGHT OF VENUS LINES, mm
|m|, ROTATIONAL LINE INDEX
0
5
10
15
20
25
30
35
40

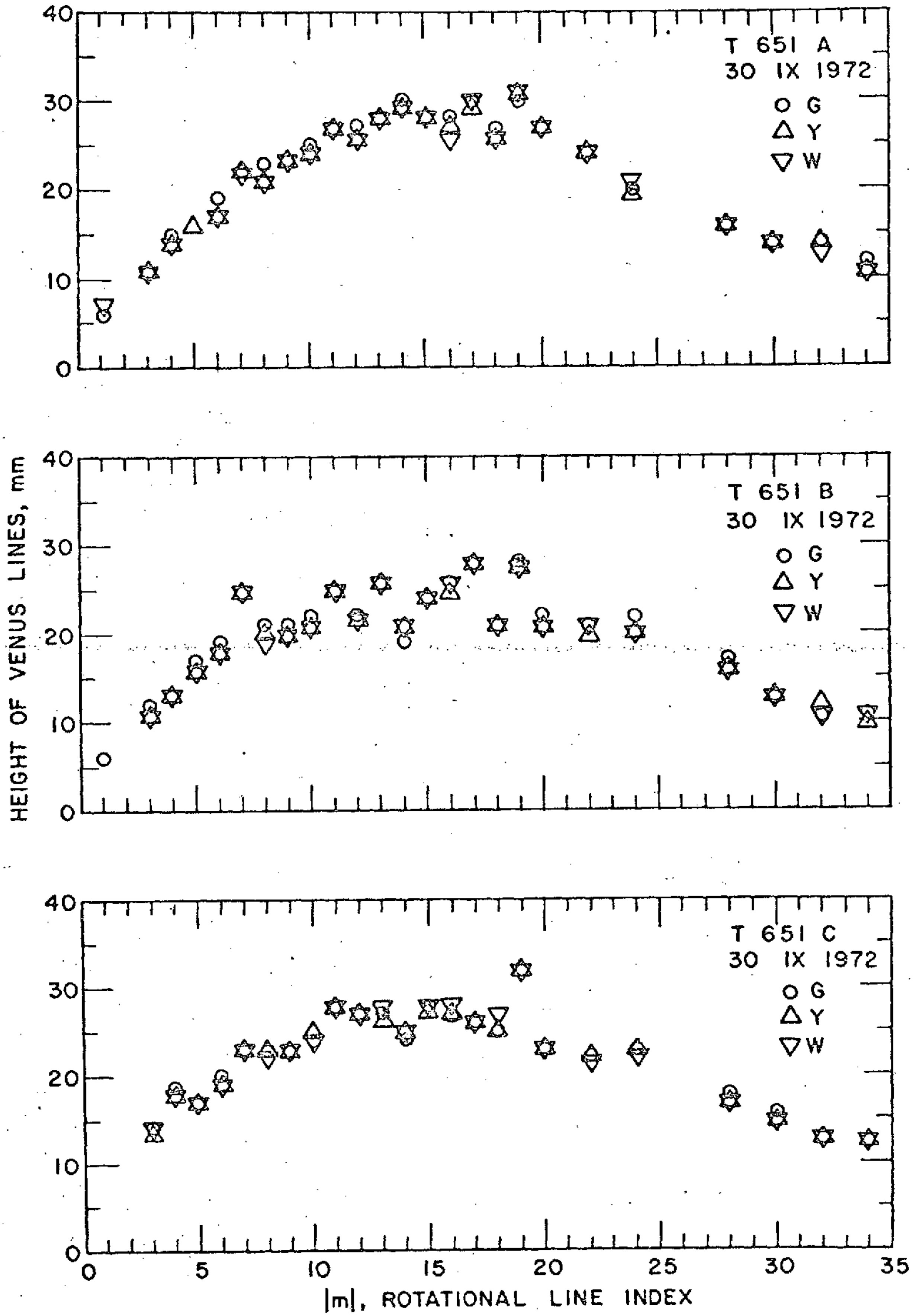

T 651 A
30 IX 1972
O G
Δ Y
∇ W
T 651 B
30 IX 1972
O G
Δ Y
∇ W
T 651 C
30 IX 1972
O G
Δ Y
∇ W
HEIGHT OF VENUS LINES, mm
|m|, ROTATIONAL LINE INDEX

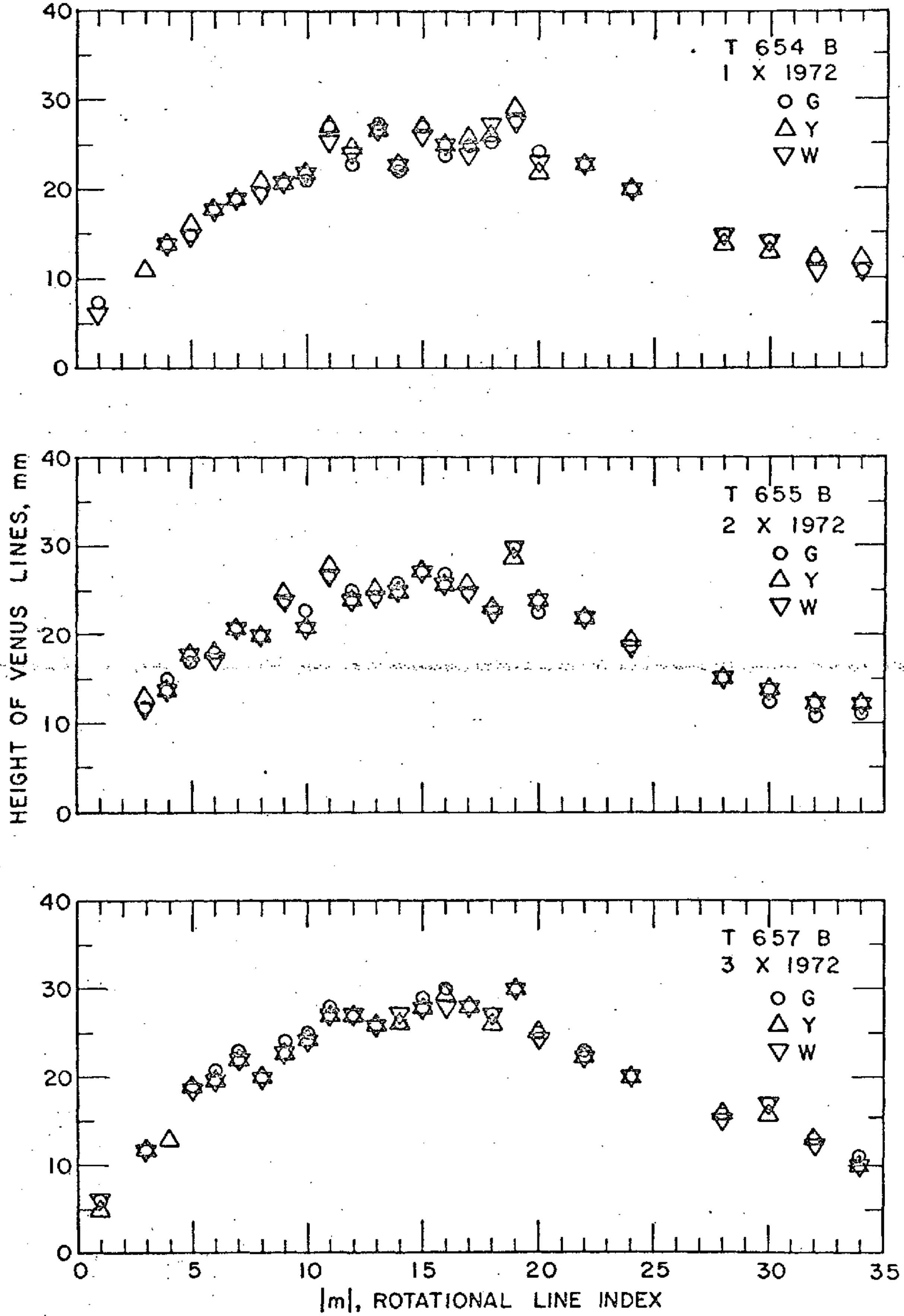

T 654 B
1 X 1972
O G
△ Y
▽ W
T 655 B
2 X 1972
O G
△ Y
▽ W
T 657 B
3 X 1972
O G
△ Y
▽ W
HEIGHT OF VENUS LINES, mm
|m|, ROTATIONAL LINE INDEX
0
5
10
15
20
25
30
35
40

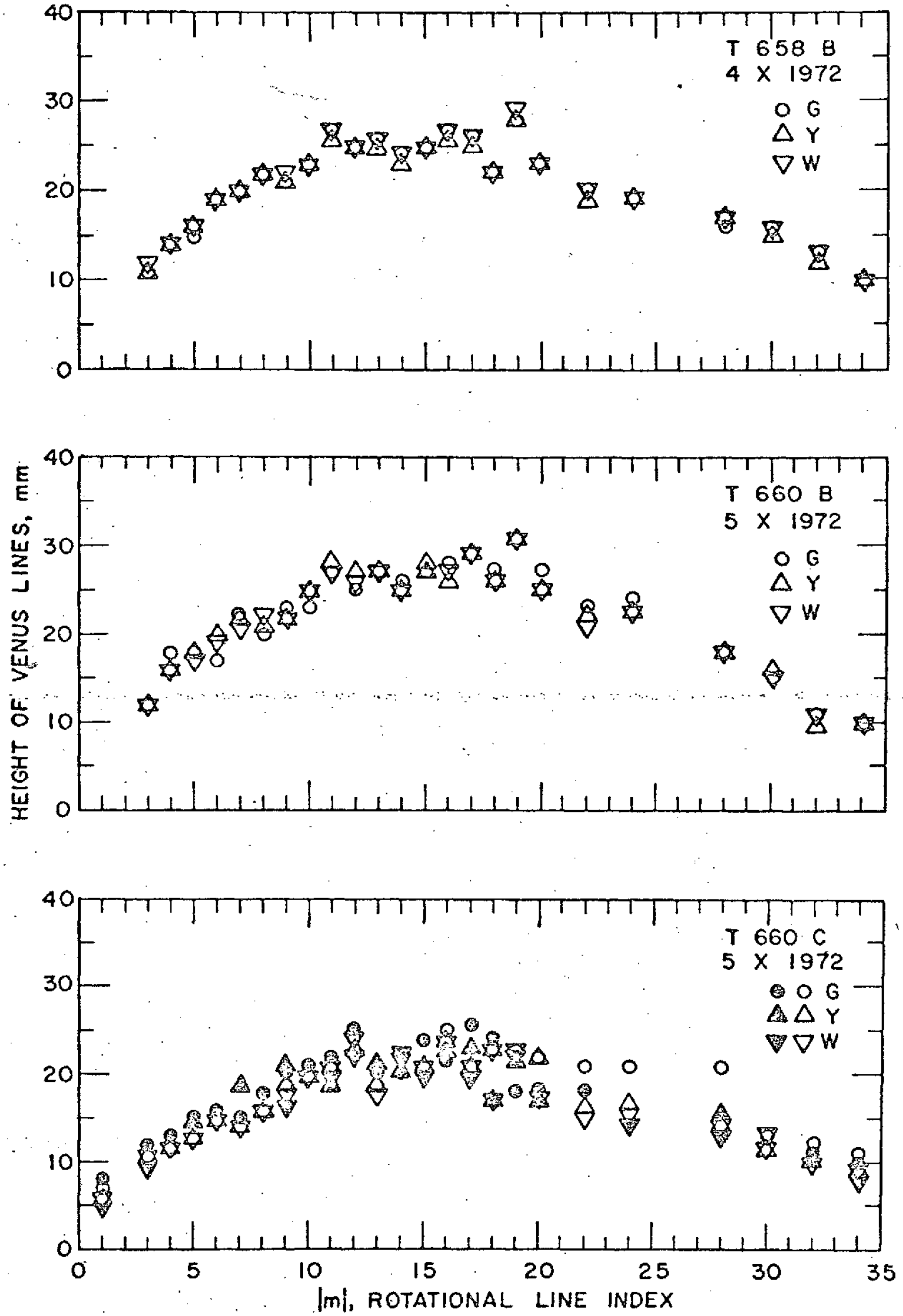
T 658 B
4 X 1972
O G
△ Y
▽ W
T 660 B
5 X 1972
O G
△ Y
▽ W
T 660 C
5 X 1972
● O G
▲ △ Y
▼ ▽ W
HEIGHT OF VENUS LINES, mm
|m|, ROTATIONAL LINE INDEX
0
10
20
30
40
0
5
10
15
20
25
30
35

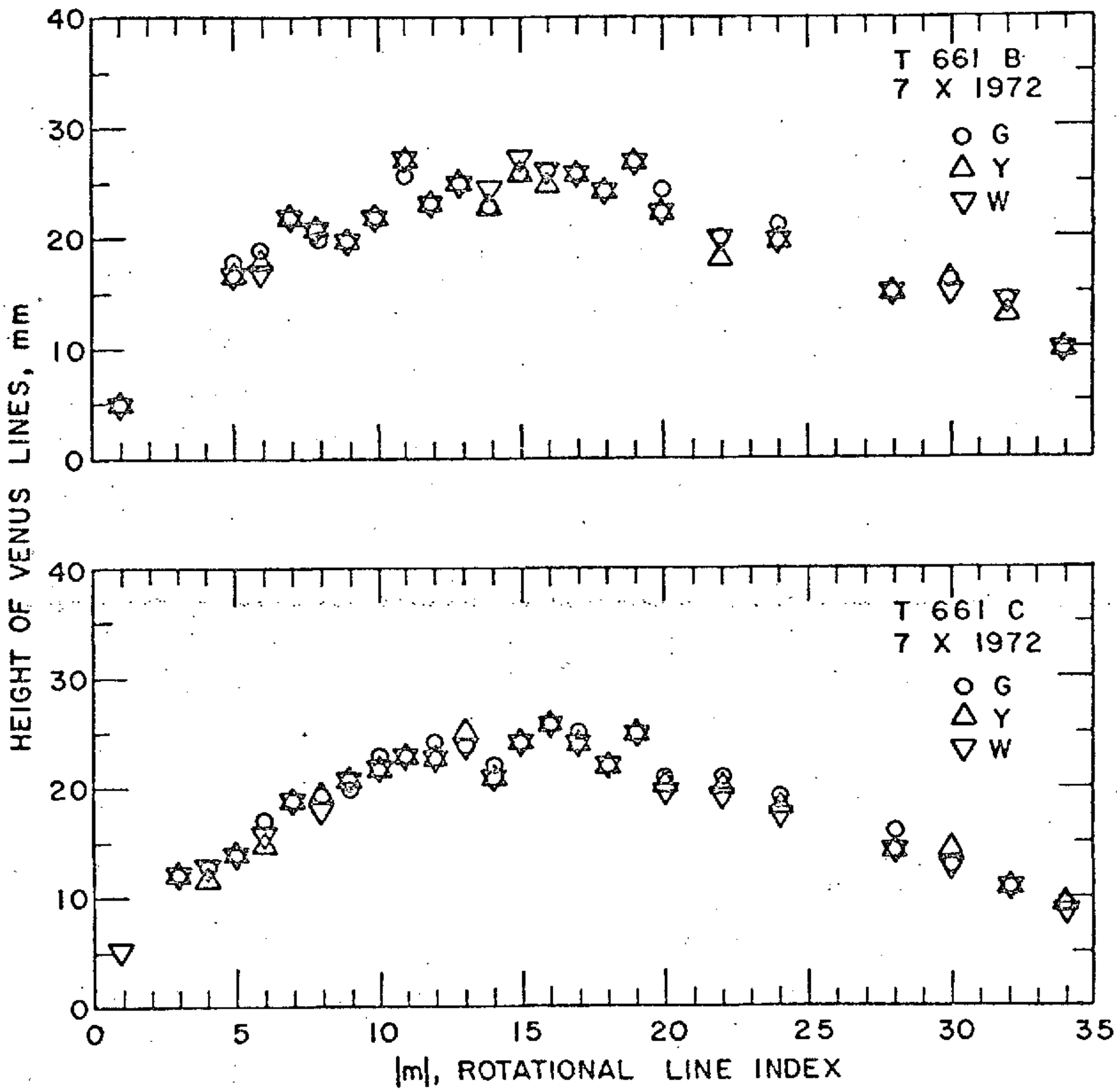

T 661 B
7 X 1972
O G
△ Y
▽ W
T 661 C
7 X 1972
O G
△ Y
▽ W
HEIGHT OF VENUS LINES, mm
0
10
20
30
40
0
5
10
15
20
25
30
35
|m|, ROTATIONAL LINE INDEX

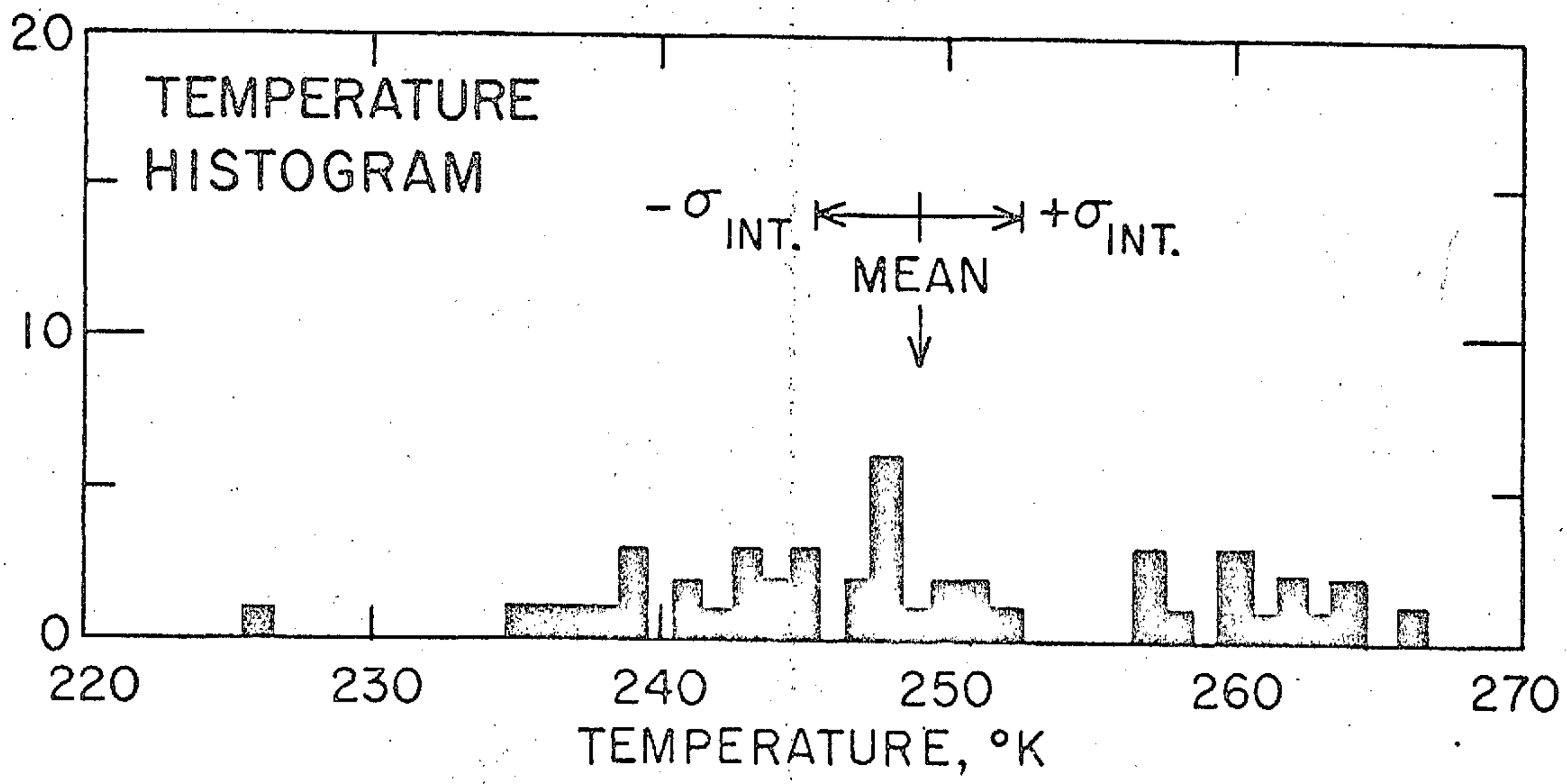

TEMPERATURE HISTOGRAM
$-\sigma_{INT.}$
$+\sigma_{INT.}$
MEAN
20
10
0
220
230
240
250
260
270
TEMPERATURE, °K

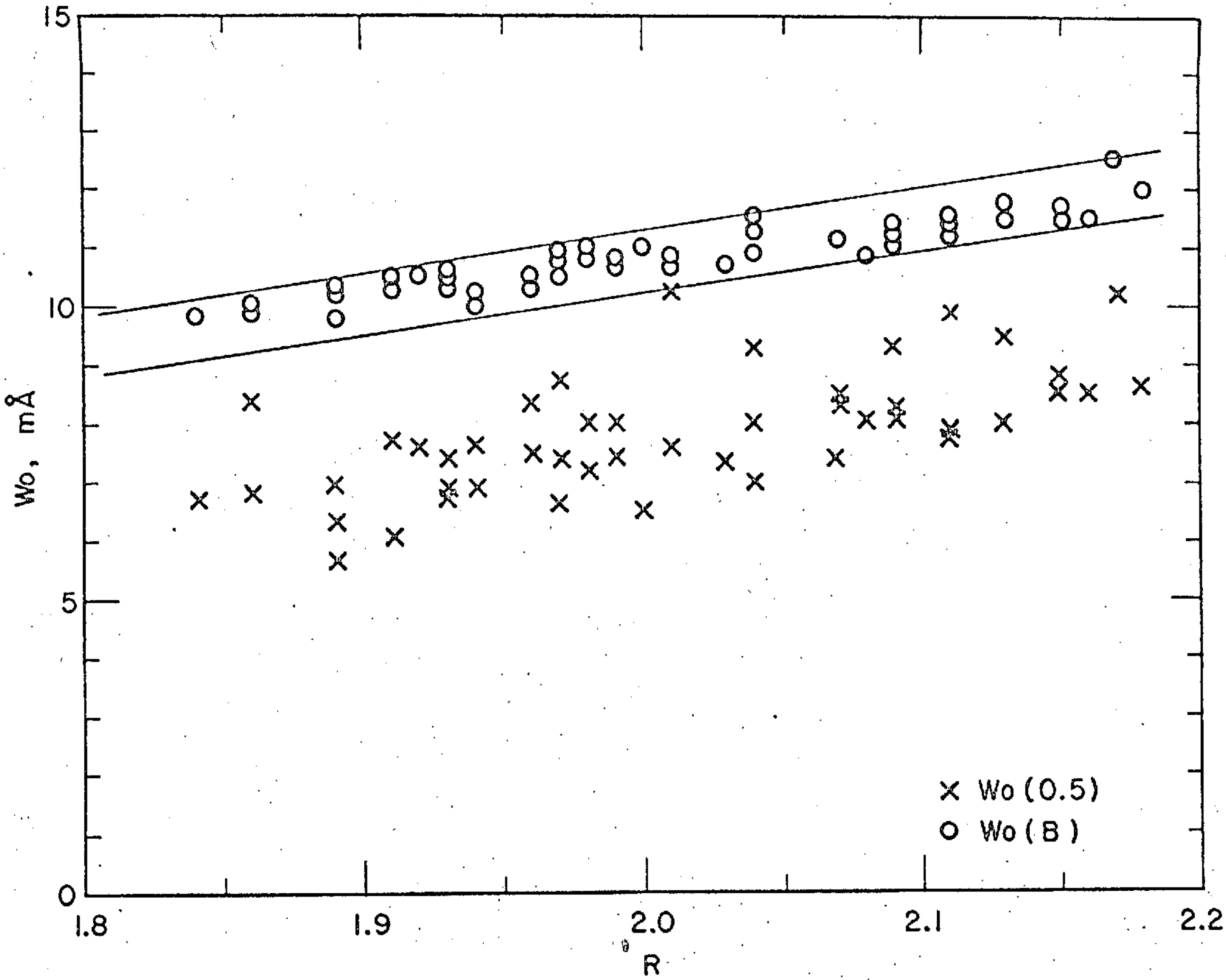

15
10
5
0
1.8
1.9
2.0
2.1
2.2
R
Wo, mÅ
Wo (0.5)
Wo (B)

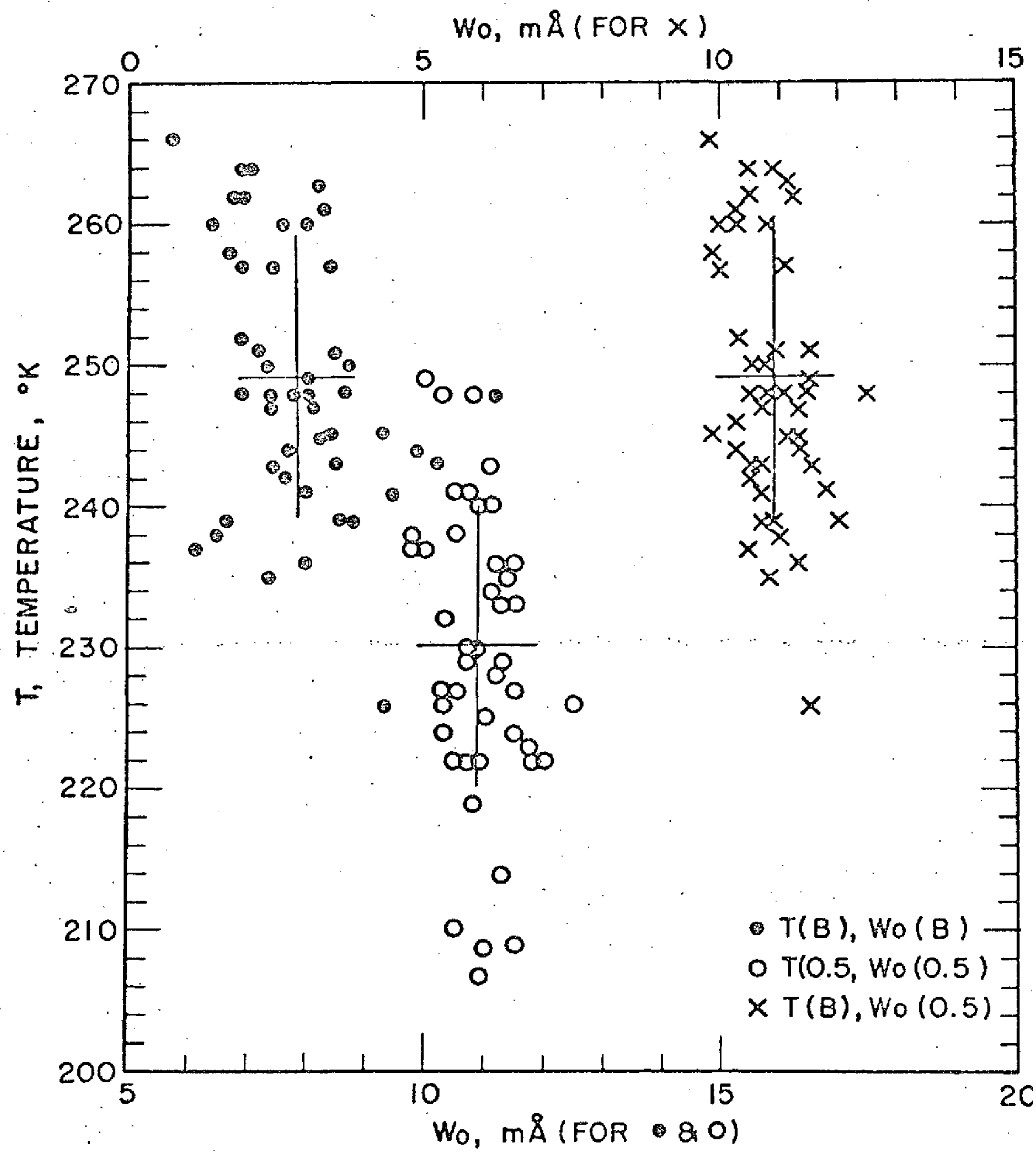

Wo, mÅ (FOR X)
0
5
10
15
270
260
250
240
230
220
210
200
T, TEMPERATURE, °K
5
10
15
20
Wo, mÅ (FOR ● & O)
● T(B), Wo (B)
O T(0.5, Wo (0.5)
X T(B), Wo (0.5)

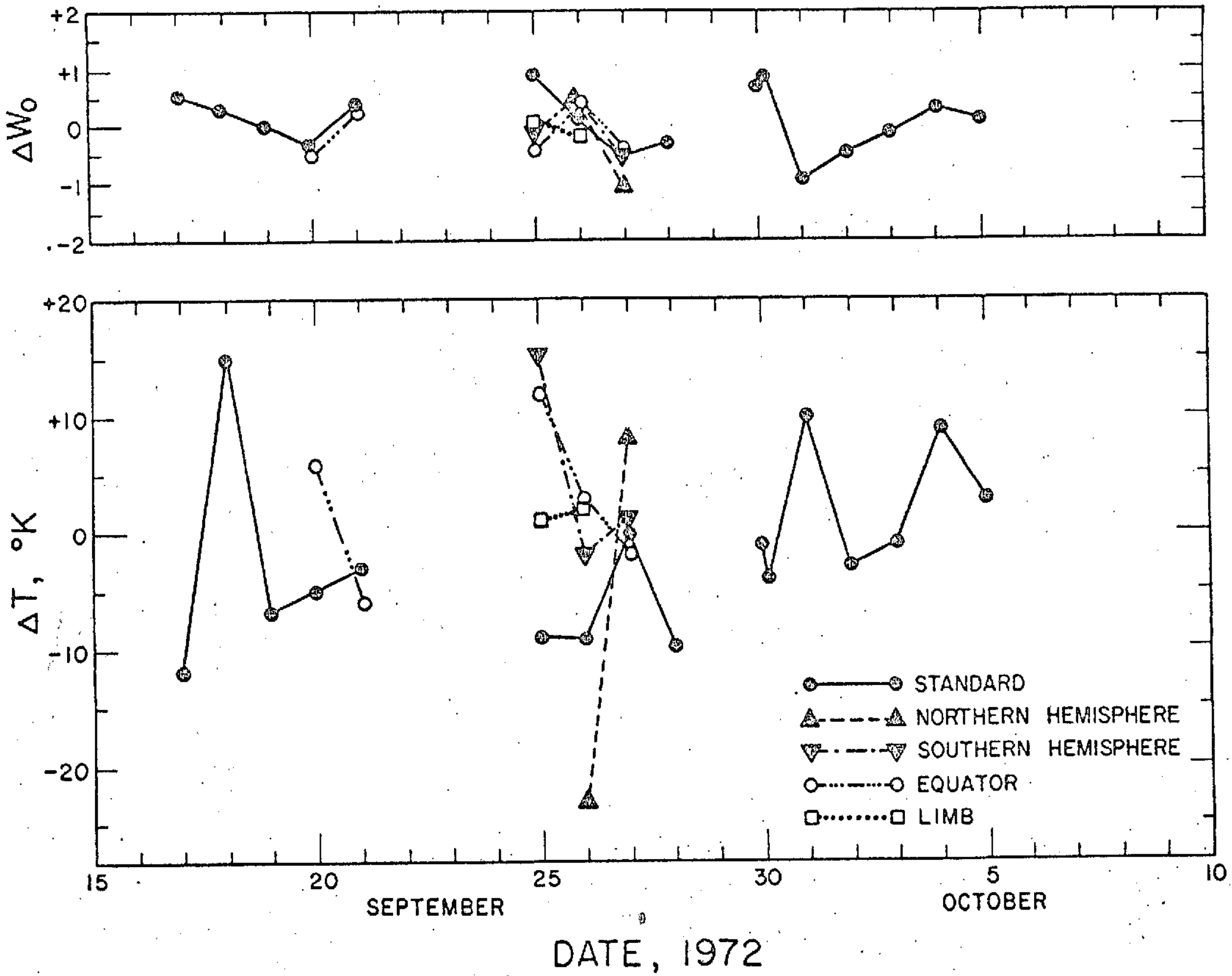

+2
+1
0
-1
-2
ΔWo
+20
+10
0
-10
-20
ΔT, °K
STANDARD
NORTHERN HEMISPHERE
SOUTHERN HEMISPHERE
EQUATOR
LIMB
15
20
25
30
5
10
SEPTEMBER
OCTOBER
DATE, 1972